The Plant Cell, Vol. 27: 675–694, March 2015, www.plantcell.org

Binding of SEC11 Indicates Its Role in SNARE Recycling after Vesicle Fusion and Identifies Two Pathways for Vesicular Traffic to the Plasma Membrane[OPEN]

Rucha Karnik,[a] Ben Zhang,[a] Sakharam Waghmare,[a] Christin Aderhold,[a] Christopher Grefen,[b] and Michael R. Blatt[a,1]

[a] Laboratory of Plant Physiology and Biophysics, University of Glasgow, Glasgow G12 8QQ, United Kingdom
[b] ZMBP Developmental Genetics, D72076 Tübingen, Germany

SNARE (soluble *N*-ethylmaleimide-sensitive factor attachment protein receptor) proteins drive vesicle fusion in all eukaryotes and contribute to homeostasis, pathogen defense, cell expansion, and growth in plants. Two homologous SNAREs, SYP121 (=SYR1/PEN1) and SYP122, dominate secretory traffic to the *Arabidopsis thaliana* plasma membrane. Although these proteins overlap functionally, differences between SYP121 and SYP122 have surfaced, suggesting that they mark two discrete pathways for vesicular traffic. The SNAREs share primary cognate partners, which has made separating their respective control mechanisms difficult. Here, we show that the regulatory protein SEC11 (=KEULE) binds selectively with SYP121 to affect secretory traffic mediated by this SNARE. SEC11 rescued traffic block by dominant-negative (inhibitory) fragments of both SNAREs, but only in plants expressing the native SYP121. Traffic and its rescue were sensitive to mutations affecting SEC11 interaction with the N terminus of SYP121. Furthermore, the domain of SEC11 that bound the SYP121 N terminus was itself able to block secretory traffic in the wild type and *syp122* but not in *syp121* mutant Arabidopsis. Thus, SEC11 binds and selectively regulates secretory traffic mediated by SYP121 and is important for recycling of the SNARE and its cognate partners.

INTRODUCTION

SNAREs (soluble *N*-ethylmaleimide-sensitive factor attachment protein receptors) comprise a highly conserved superfamily of proteins that mediate in the traffic of vesicles between endosomal compartments as well as in secretory traffic to the plasma membrane in all eukaryotic cells. SNAREs drive the fusion of vesicle and target membranes and enable the transfer of soluble and membrane-associated cargos in a highly regulated manner (Pratelli et al., 2004; Jahn and Scheller, 2006; Lipka et al., 2007; Bassham and Blatt, 2008). In plant cells, SNARE-mediated vesicle traffic delivers wall materials and membrane to the cell surface, making essential contributions to homeostasis, cell expansion, and growth (Blatt, 2000; Shope et al., 2003; Campanoni and Blatt, 2007). It also plays important roles in resistance to pathogens (Kalde et al., 2007; Zhang et al., 2007) and responses to abiotic stress (Grefen and Blatt, 2008; Eisenach et al., 2012). Cognate SNAREs localize to vesicle and target membranes, and during the SNARE cycle, their assembly in a stable heteromeric core complex draws vesicle and target membranes together for fusion of the two bilayers. Each SNARE in the complex contributes one or more of a set of highly conserved motifs, classified according to their structure and the amino acid (Q [Gln] or R [Arg]) present at the center of the motif (Fasshauer et al., 1998; Bock et al., 2001). Qa-SNAREs generally localize to the target membrane along with Qb- and Qc-SNAREs, or with Qbc-SNAREs that are often referred to as SNAP25-related (synaptosome-associated protein of 25 kD) proteins; R-SNAREs are present on the vesicle membrane and are also known as VAMPs (vesicle-associated membrane proteins).

Plants display the widest spatiotemporal and developmental distribution of SNAREs among eukaryotes (Sanderfoot et al., 2000; Pratelli et al., 2004), reflecting the need for specialized functions throughout the life cycle of the plant (Bassham and Blatt, 2008; Grefen and Blatt, 2008). The Qa-SNAREs of the plasma membrane are a case in point. In *Arabidopsis thaliana*, two of these SNAREs, SYP121 (=SYR1/PEN1) and SYP122, show a high degree of structural homology and overlap in function (Assaad et al., 2004; Tyrrell et al., 2007; Bassham and Blatt, 2008; Rehman et al., 2008). Single mutations of these Qa-SNAREs have little effect on plant growth under many conditions, and reduced growth is normally evident only in the *syp121/syp122* double mutant (Assaad et al., 2004; Zhang et al., 2007). Both SYP121 and SYP122 are expressed throughout the development of the plant and in most, if not all, tissues (Uemura et al., 2004; Enami et al., 2009). The Qa-SNAREs also share the cognate partner proteins SNAP33, VAMP721, and VAMP722 (Kwon et al., 2008; Rehman et al., 2008; Karnik et al., 2013b), indicating substantial mechanistic overlaps in driving vesicle fusion. Nonetheless, a number of functional differences between SYP121 and SYP122 have surfaced. SYP121 has unique roles in responses to drought and the water stress hormone abscisic acid (Leyman et al., 1999; Sutter et al., 2007; Eisenach et al., 2012), and it facilitates targeted vesicle traffic for defense against pathogen attack (Kwon et al., 2008). Furthermore, SYP121 uniquely interacts with K^+ channels to facilitate the uptake

[1] Address correspondence to michael.blatt@glasgow.ac.uk.
The author responsible for distribution of materials integral to the findings presented in this article in accordance with the policy described in the Instructions for Authors (www.plantcell.org) is: Michael R. Blatt (michael.blatt@glasgow.ac.uk).
[OPEN]Articles can be viewed online without a subscription.
www.plantcell.org/cgi/doi/10.1105/tpc.114.134429

of the solute for cell expansion and plant growth (Honsbein et al., 2009, 2011; Grefen et al., 2010a). These observations raise the most fundamental questions about the nature of the regulation that could give rise to their distinctive roles in vesicle traffic and its control, and they highlight our relative ignorance generally about the vesicle-trafficking pathways to the plasma membrane mediated by SYP121 and SYP122.

Clues to the molecular mechanics regulating SYP121 have come from recent studies of SEC11 (=KEULE), a member of the Sec1/Munc18 (SM) protein family (Südhof and Rothman, 2009; Hughson, 2013) that, in animals and yeast, regulate Qa-SNARE availability for SNARE complex assembly and stabilize the complex during vesicle fusion. SEC11 was originally identified as a binding partner of the Qa-SNARE SYP111 (=KNOLLE) that is expressed and functions only during cytokinesis (Waizenegger et al., 2000; Assaad et al., 2001; Park et al., 2012). Nonetheless, SEC11 is expressed throughout the vegetative plant and not just during cell division. Karnik et al. (2013b) demonstrated that SEC11 will bind with SYP121 and regulate its activity at the plasma membrane. Significantly, SEC11 binding to the N terminus of SYP121 affected binary interaction with the Qa-SNARE but not its assembly in the SNARE core complex. These findings highlighted a role for SEC11 unlike that of SM proteins in animals, and they offered a strategy with which to explore potential differences in traffic control mediated through SYP121 and SYP122.

Here, we set out this strategy using SEC11 and its N-terminal fragment that binds SYP121 to probe secretory traffic in Arabidopsis. We report that SEC11 interacted selectively with SYP121 over SYP122 in vitro and when expressed in yeast and that it rescued secretory traffic block in the *syp122*, but not in the *syp121*, mutant in vivo. The N-terminal fragment of SEC11 itself inhibited secretion, but only in plants expressing SYP121. These and additional results underscore the specificity of SEC11 in regulating traffic to the plasma membrane mediated by SYP121 and, most importantly, they point to a role for SEC11 in recycling of the SNARE complex after vesicle fusion.

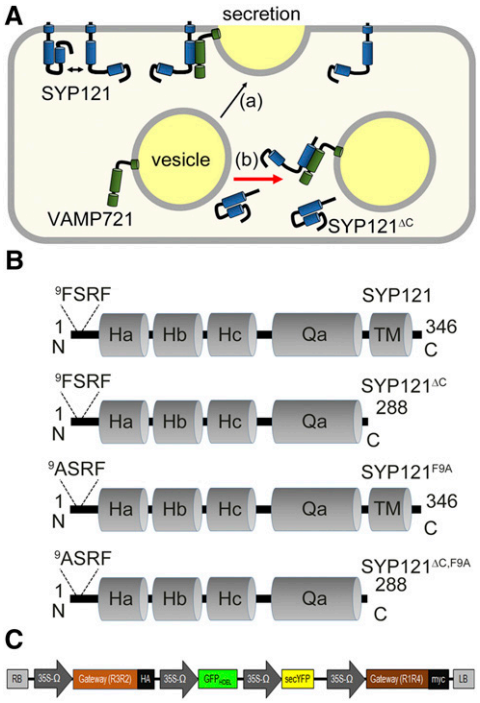

Figure 1. Schematics of SYP121, Its Cytosolic Fragments, and Their Proposed Block of Secretory Traffic.

(A) Schematic of secretory traffic block by SYP121$^{\Delta C}$. For simplicity, only SYP121 and the R-SNARE VAMP721 are shown. Path a shows normal traffic leading to vesicle fusion at the plasma membrane mediated by SYP121 and VAMP721. Path b shows the soluble SYP121$^{\Delta C}$ fragment binding VAMP721, thereby competing with SYP121-mediated traffic.
(B) Schematics of full-length SYP121 and SYP121^{F9A} and for the SYP121$^{\Delta C}$ and SYP121$^{\Delta C,F9A}$ fragments, showing the domain organization and location of the FxRF motif at the SYP121 N terminus.
(C) Schematic of the tetracistronic vector pTecG-2in1-CC, incorporating coding sequences for secYFP and GFP-HDEL for assay of secretion and cassettes for the expression of a further two proteins.

RESULTS

Qa-SNARE Fragments SYP121$^{\Delta C}$ and SYP122$^{\Delta C}$ Block Secretory Traffic

The cytosolic fragments of the Qa-SNAREs SYP121$^{\Delta C}$ (=SYP121-Sp2) and SYP122$^{\Delta C}$ (=SYP122-Sp2) were shown previously to block secretion at a stage late in transit to the plasma membrane in tobacco (*Nicotiana tabacum*) and Arabidopsis (Geelen et al., 2002; Sutter et al., 2006; Tyrrell et al., 2007; Besserer et al., 2012; Karnik et al., 2013b). Secretory block was proposed (Figure 1A) to arise by the titration of cognate SNARE partners, thus accounting for the lack of selectivity between the cytosolic fragments (Tyrrell et al., 2007), but this interpretation was not addressed directly using the complementary mutant backgrounds. We expressed the fluorescent secretory marker secreted yellow fluorescent protein (secYFP) and the endoplasmic reticulum marker GFP-HDEL with and without SYP121$^{\Delta C}$ (Figure 1B) and SYP122$^{\Delta C}$ using the tetracistronic vector pTecG-2in1-CC (Figure 1C) (Karnik et al., 2013b) to transiently transform Arabidopsis Columbia-0 (wild type), *syp121-1* (*syp121*), and *syp122-1* (*syp122*) mutant seedlings (Zhang et al., 2007; Honsbein et al., 2009; Grefen et al., 2010b). secYFP is exported from the cell and normally yields little or no fluorescence once in the apoplast. Thus, only secYFP retained in the cell fluoresces strongly. Coexpression of the endoplasmic reticulum marker GFP-HDEL allowed transformations to be verified on a cell-by-cell basis and enabled the quantification of secYFP retention as the ratio of yellow fluorescent protein (YFP) to green fluorescent protein (GFP) fluorescence in the tissue.

Cocultivation with *Agrobacterium tumefaciens* normally gives a strong transformation of the root epidermis (Honsbein et al., 2009; Grefen et al., 2010b; Karnik et al., 2013b). Therefore, we quantified secYFP traffic by confocal microscopy of seedling roots, using standardized excitation and emission settings, and analyzed 3D projections for YFP and GFP fluorescence after subtracting background fluorescence signals recorded from untransformed seedlings. Figure 2A shows images from one set of transformations and includes immunoblot analysis for the expression of the Qa-SNARE fragments. Figure 2B summarizes the results from all experiments ($n \geq 15$ for each data set). In

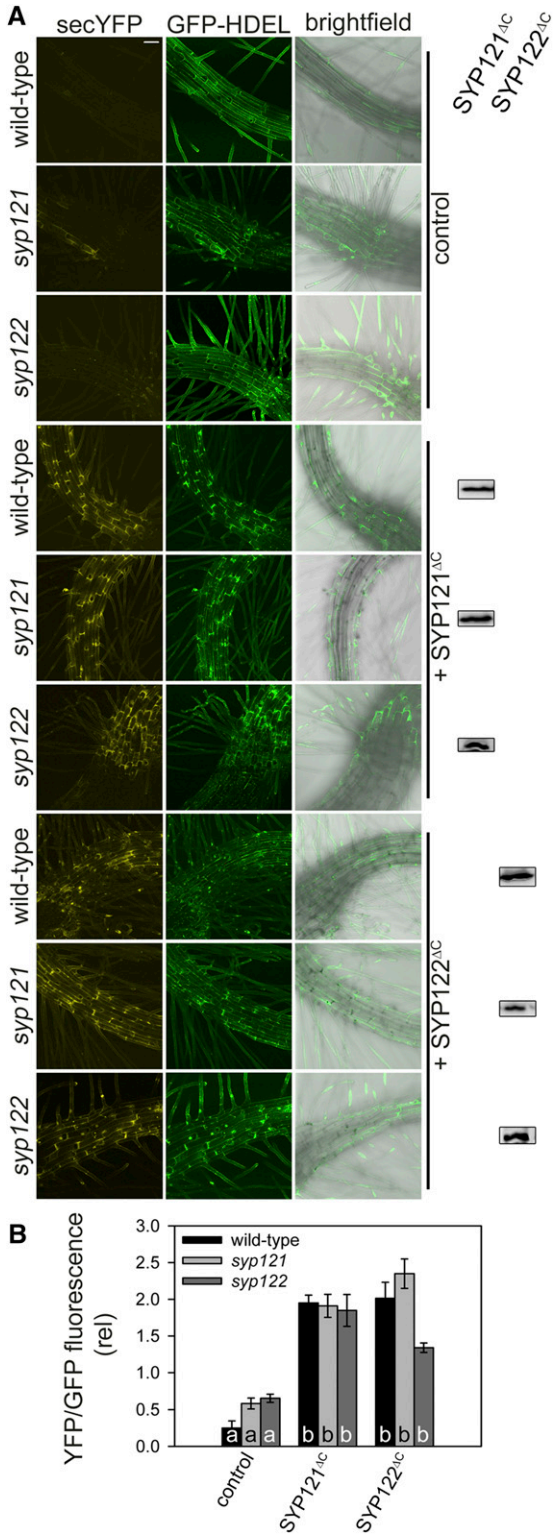

Figure 2. SYP121$^{\Delta C}$ and SYP122$^{\Delta C}$ Fragments Block Secretion in Wild-Type, *syp121*, and *syp122* Arabidopsis.

(A) Representative confocal images (left to right) of fluorescence from the secretory marker secYFP and the retained (endoplasmic reticulum) marker GFP-HDEL rendered as 3D projections, along with the corresponding, mid-stack merged bright-field and GFP-HDEL image. Images are of transiently transformed wild-type, *syp121*, and *syp122* Arabidopsis seedlings (indicated at left) expressing secYFP and GFP-HDEL alone (control) and together with SYP121$^{\Delta C}$ and SYP122$^{\Delta C}$ (indicated at right). Immunoblot analysis verifying the expression of SYP121$^{\Delta C}$ and SYP122$^{\Delta C}$ using anti-myc antibody is shown at right. Bar = 50 μm.

(B) secYFP:GFP-HDEL fluorescence ratios as means ± SE of >15 independent experiments for each construct and Arabidopsis line. Fluorescence ratios were calculated as the mean tissue fluorescence determined from 3D projections of root images after correcting for the background fluorescence similarly recorded from untransformed seedlings of the same age. Significance is indicated by lettering at $P < 0.05$.

every case, seedlings transformed with secYFP and GFP-HDEL alone showed a low ratio of YFP to GFP fluorescence, typically around 0.5 or less, regardless of the genetic background of the seedlings. A small increase in the mean YFP:GFP ratio was observed in measurements from the *syp121* and *syp122* mutants when compared with the wild-type seedlings, but the difference was not significant. Coexpression with SYP121$^{\Delta C}$ and SYP122$^{\Delta C}$ yielded substantial increases in the YFP:GFP ratio, indicating the retention of secYFP, again regardless of the genetic background. We noted a small difference between the mutant backgrounds only when comparing the YFP:GFP ratios on SYP122$^{\Delta C}$ coexpression, suggesting that this Qa-SNARE fragment was more effective in blocking secYFP export in the *syp121* mutant. Again, the difference between the genetic backgrounds was not very significant, and SYP121$^{\Delta C}$ was equally effective in retaining secYFP in all three Arabidopsis lines. These findings support the interpretation of a common pool of interacting partners shared by the two Qa-SNAREs.

SEC11 Rescues Secretory Block in *syp122* but Not in *syp121* Mutant Plants

Although SEC11 rescues traffic block by SYP121$^{\Delta C}$ in tobacco (Karnik et al., 2013b), these earlier findings do not distinguish between two general mechanisms. Expressing SEC11 might rescue traffic by binding with and sequestering the SYP121$^{\Delta C}$ fragment, preventing its actions either in the cytosol or at the plasma membrane; alternatively, SEC11 rescue might reflect a genuine facilitation of vesicle fusion through its interaction with the native SYP121 in Arabidopsis or its homolog at the plasma membrane in tobacco. To distinguish between these two possibilities, we used the pTecG-2in1-CC vector to coexpress secYFP and GFP-HDEL with SEC11 alone and together with the two Qa-SNARE fragments. Again, experiments were performed in Arabidopsis wild-type, *syp121*, and *syp122* seedlings, and image data were quantified using the YFP:GFP fluorescence ratio. Figure 3A includes the results from one set of transformations along with immunoblot analysis for the expression of the Qa-SNARE fragments and SEC11. The results of all of the experiments are summarized in Figure 3B. (These and the subsequent studies were run in parallel with the data of Figure 2. The latter are included here and in the subsequent figures for visual comparison.) We found that expressing SEC11 on its own

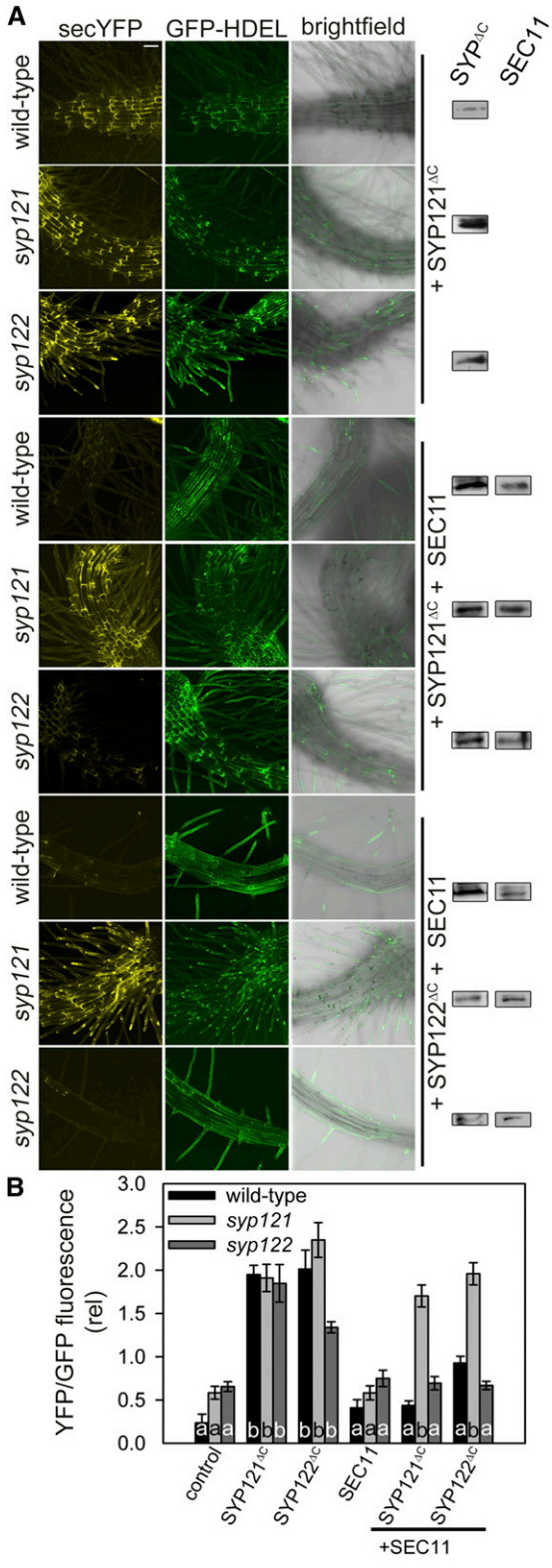

Figure 3. SEC11 Rescues Secretory Block in Wild-Type and *syp122*, but Not in *syp121*, Arabidopsis.

had no measurable effect on secYFP traffic when assayed in this fashion (Karnik et al., 2013b). Coexpressing SEC11 with SYP121$^{\Delta C}$ and SYP122$^{\Delta C}$ rescued traffic block by the Qa-SNARE fragments in the wild-type and *syp122* mutant seedlings. In the *syp121* mutant, however, SEC11 coexpression was without effect in reducing the YFP:GFP ratios when compared with those determined for seedlings expressing SYP121$^{\Delta C}$ or SYP122$^{\Delta C}$ alone. We concluded that SEC11 is able to rescue secYFP traffic, irrespective of the Qa-SNARE fragment, provided that the native SYP121 is expressed. In short, the results argue against SEC11 titration of SYP121$^{\Delta C}$ and SYP122$^{\Delta C}$ in the cytosol, instead implicating a direct and selective interaction with SYP121 at the plasma membrane.

To test SEC11 selectivity between the two full-length Qa-SNAREs, we used a modified version of the yeast mating-based split-ubiquitin (SUS) assay (Grefen et al., 2010a; Grefen and Blatt, 2012b; Grefen, 2014). SUS assays are useful to test interactions between membrane-anchored proteins. One requirement of the SUS approach is that the bait protein be membrane anchored so that the bait construct cannot migrate to the nucleus on its own to activate the reporter gene in the absence of prey interaction. The CytoSUS assay overcomes this limitation, incorporating, as an N-terminal anchor for a soluble bait construct, the integral membrane protein subunit of the yeast oligosaccharyltransferase complex of the endoplasmic reticulum lumen (OST4p) (Möckli et al., 2007). We designed a Gateway-compatible SUS bait vector with this construct, here designated mOST4, to give expression with SEC11. Diploid yeast expressing SYP121 or SYP122 as the prey protein with mOST4-SEC11 as the bait protein were obtained as before by mating and growth on synthetic medium lacking leucine, tryptophan, uracil, and methionine. Expression of the bait is under methionine promoter repression; therefore, methionine was used to test for interaction specificity. The results (Supplemental Figure 1) showed that growth on selective medium was retained in yeast expressing mOST4-SEC11 and SYP121, even in the presence of 50 and 500 μM methionine, but little or no growth was found with yeast expressing the bait with SYP122 under the same conditions.

(A) Representative confocal images (left to right) of fluorescence from the secretory marker secYFP and the retained (endoplasmic reticulum) marker GFP-HDEL rendered as 3D projections, along with the corresponding, mid-stack merged bright-field and GFP-HDEL image. Images are of transiently transformed wild-type, *syp121*, and *syp122* Arabidopsis seedlings (indicated at left) expressing secYFP and GFP-HDEL with SYP121$^{\Delta C}$ and SYP122$^{\Delta C}$ alone and together with SEC11 (indicated at right). Immunoblot analysis verifying the expression of SYP121$^{\Delta C}$, SYP122$^{\Delta C}$, and SEC11 using anti-myc and anti-HA antibodies, respectively, is shown at right. Controls with secYFP and GFP-HDEL alone and with SYP122$^{\Delta C}$ are found in Figure 2. Bar = 50 μm.

(B) secYFP:GFP-HDEL fluorescence ratios as means ± SE of more than five independent experiments for each construct and Arabidopsis line. Fluorescence ratios were calculated as the mean tissue fluorescence determined from 3D projections of root images after correcting for the background fluorescence similarly recorded from untransformed seedlings of the same age. Significance is indicated by lettering at $P < 0.05$. Data for SYP122$^{\Delta C}$ have been omitted from the graph for clarity (see Figure 2B).

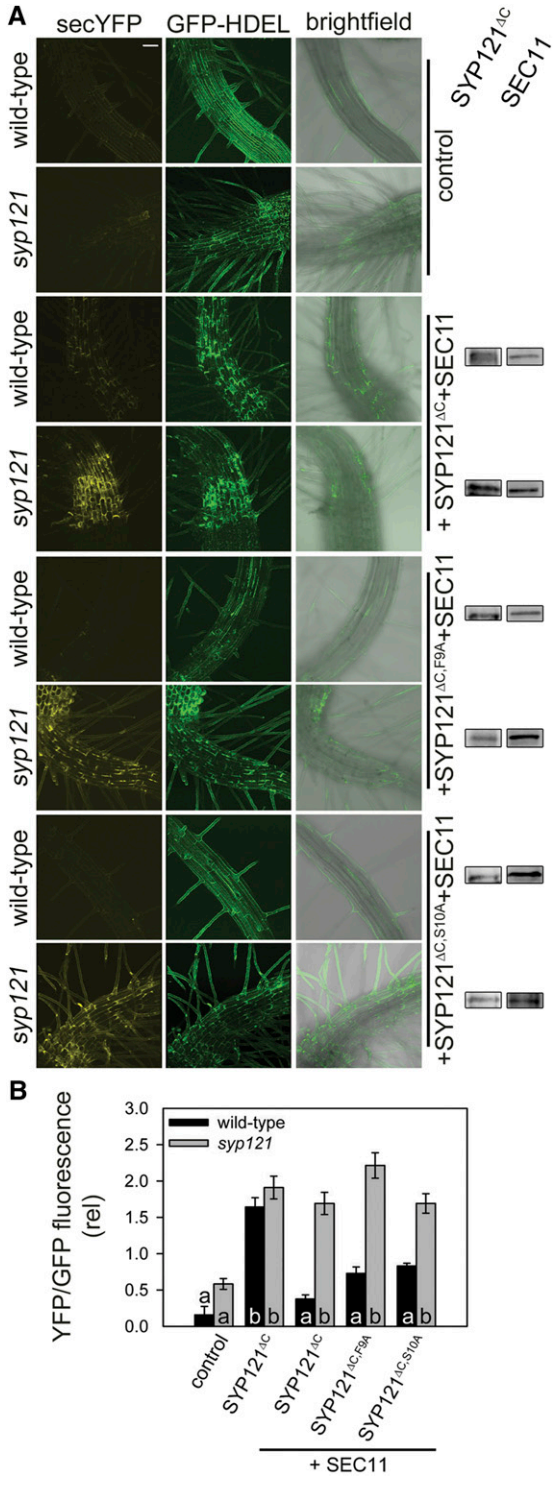

Figure 4. SEC11 Rescues Secretory Traffic Independent of Phe-9 Substitution in SYP121$^{\Delta C,F9A}$, but Only in the Presence of the Native SYP121.

(A) Representative confocal images (left to right) of fluorescence from the secretory marker secYFP and the retained (endoplasmic reticulum) marker GFP-HDEL rendered as 3D projections, along with the corresponding, mid-stack merged bright-field and GFP-HDEL image. Images are of transiently transformed wild-type and *syp121* Arabidopsis seedlings (indicated at left) expressing secYFP and GFP-HDEL alone (control) and with each of the soluble fragments SYP121$^{\Delta C}$, SYP121$^{\Delta C,F9A}$, and SYP121$^{\Delta C,S10A}$ together with SEC11 (indicated at right). Immunoblot analysis verifying the expression of the Qa-SNARE fragments and SEC11 using anti-myc and anti-HA antibodies, respectively, is shown at right. Controls with secYFP and GFP-HDEL with SYP121$^{\Delta C}$ are found in Figure 2. Bar = 50 μm.

(B) secYFP:GFP-HDEL fluorescence ratios as means ± SE of more than five independent experiments for each construct and Arabidopsis line. Fluorescence ratios were calculated as the mean tissue fluorescence determined from 3D projections of root images after correcting for the background fluorescence similarly recorded from untransformed seedlings of the same age. Significance is indicated by lettering at $P < 0.05$.

These data are consistent with the findings of *syp121*-sensitive traffic rescue, confirming a selectivity of SEC11 for interaction with SYP121.

Traffic Rescue Is Not Dependent on SEC11 Binding with the N Terminus of SYP121$^{\Delta C}$

Phe-9 is highly conserved among many Qa-SNAREs of animals, yeast, and *Drosophila melanogaster*; it is critical for SM protein binding to regulate SNARE core complex assembly (Bracher and Weissenhorn, 2002; Burgoyne and Morgan, 2007; Südhof and Rothman, 2009), and it is present in SYP121 (Grefen et al., 2010a). Karnik et al. (2013b) found that the SYP121^{F9A} mutation suppressed SEC11 binding to the SYP121 N terminus and eliminated the ability of SEC11 to stabilize the so-called "closed" conformation of SYP121 against assembly with its cognate SNARE partners in vitro. We used this knowledge to test whether SEC11 binding to this domain of SYP121 contributed to traffic rescue by the SM protein. We generated mutants of the Qa-SNARE soluble fragment incorporating the Phe substitution (SYP121$^{\Delta C,F9A}$) and, as a control, the equivalent substitution in the adjacent Ser residue (SYP121$^{\Delta C,S10A}$), using the pTecG-2in1-CC vector to transform wild-type and *syp121* mutant Arabidopsis as before. The results (Supplemental Figure 2) showed that expressing the soluble fragments SYP121$^{\Delta C}$, SYP121$^{\Delta C,F9A}$, and SYP121$^{\Delta C,S10A}$ each yielded a similar retention of secYFP and elevated the YFP:GFP ratio, both in wild-type and *syp121* mutant seedlings, indicating that Phe-9 of the SYP121$^{\Delta C}$ fragment does not contribute to traffic block.

We next assessed whether SEC11 was similarly effective in rescuing traffic blocked by the soluble SYP121$^{\Delta C,F9A}$ fragment as it was when block was achieved with SYP121$^{\Delta C}$. We reasoned that if SEC11 binding to the Qa-SNARE fragment N terminus was important for its rescue of traffic, such as might result from stabilizing the closed state of SYP121$^{\Delta C}$, then secYFP traffic rescue should be lost when SEC11 was coexpressed with the SYP121$^{\Delta C,F9A}$ mutant. Figure 4 summarizes experiments in which SYP121$^{\Delta C}$, SYP121$^{\Delta C,F9A}$, and SYP121$^{\Delta C,S10A}$ were coexpressed with SEC11 in wild-type and *syp121* mutant seedlings. In wild-type Arabidopsis, the fluorescence ratios on SEC11 coexpression with each of the soluble fragments SYP121$^{\Delta C}$, SYP121$^{\Delta C,F9A}$, and SYP121$^{\Delta C,S10A}$ were reduced significantly, consistent with SEC11 rescue of secYFP secretion. In the *syp121* mutant plants, secYFP retention and the fluorescence ratios were comparable to the signals when

SYP121$^{\Delta C}$ was expressed alone, regardless of the mutation in the Qa-SNARE fragment. These data, like the results of Figure 3, demonstrate a requirement for the native SYP121. Additionally, they show that traffic rescue by the full-length SEC11 cannot be explained by its putative interaction with the N terminus of SYP121$^{\Delta C}$.

SEC11 Interaction with the N Terminus of SYP121 at the Plasma Membrane Is Important for Secretion and Traffic Rescue

To test if SEC11 interaction with the native SYP121 N terminus contributes to the rescue of vesicle traffic, we examined secYFP retention in *syp121* mutant Arabidopsis stably complemented to express the full-length mutant SYP121^{F9A} under the control of the constitutive Ubiquitin-10 promoter (*syp121*:*SYP121*^{F9A}) (Karnik et al., 2013b). Seedlings of *syp121*:*SYP121*^{F9A} plants were transiently transformed to quantify secYFP and GFP-HDEL fluorescence as before. For comparison, we include data for parallel transformations of wild-type and *syp121* mutant plants in Figure 5. Image analysis showed enhanced secYFP fluorescence and roughly a 5-fold increase in the YFP:GFP fluorescence ratio in the *syp121*:*SYP121*^{F9A} seedlings expressing the full-length mutant SYP121^{F9A} when compared with the wild-type control, even when only the secYFP and GFP-HDEL constructs were expressed (Figures 5A and 5B, control). The elevated fluorescence ratio was statistically indistinguishable from the ratios observed on coexpressing the SYP121$^{\Delta C}$ fragment. Coexpression with SEC11 had no added effect in elevating the fluorescence ratio in the *syp121*:*SYP121*^{F9A} complemented plants. These results indicated that disrupting SEC11 binding to the N terminus of the full-length Qa-SNARE alone was sufficient to suppress secYFP traffic.

SEC11, like other SM proteins (Südhof and Rothman, 2009; Hughson, 2013), is thought to form a clothespeg-like structure that clamps the SNARE complex once assembled within its major cleft, thereby stabilizing the complex for vesicle fusion. SEC11 binding with the SYP121 N terminus tethers the two proteins (Park et al., 2012). It favors a quasi-open conformation of SYP121 that is not fusion competent; only together with additional regulatory factors is SEC11 thought to convert SYP121 to an "open" conformation ready for SNARE complex assembly (Karnik et al., 2013b). SEC11 binding to the SYP121 N terminus is affected by mutations within a minor cleft thought to form at the surface of the N-terminal half of SEC11. Introducing the positively charged Arg residue in the SEC11^{L128R} mutant abolishes SEC11 binding with the SYP121 N terminus but does not affect SM protein binding to the SNARE complex assembled of SYP121, SNAP33, and VAMP721 (Karnik et al., 2013b). We hypothesized that if binding with SYP121 in the complex was important for traffic rescue at the plasma membrane, then expressing SEC11^{L128R}, which eliminates tethering but not binding to the SNARE complex, should nonetheless rescue secYFP traffic.

To test SEC11^{L128R} interaction with the full length SYP121, again we used the mOST4-anchored SEC11 in the SUS assay with the Qa-SNARE. Diploid yeast expressing SYP121 as the prey protein with either mOST4-SEC11 or mOST4-SEC11^{L128R} as the bait protein were obtained and grown as before (Grefen et al., 2010a; Grefen and Blatt, 2012a). Figure 6 shows that growth on selective medium was retained in yeast expressing mOST4-SEC11 and SYP121, even in the presence of 50 and 500 μM methionine, concentrations that yielded little or no growth of diploid yeast expressing mOST4-SEC11^{L128R} and SYP121. These data indicated that the SEC11^{L128R} mutation suppresses its binding with the full-length SYP121 protein. Thus, the SEC11^{L128R} mutant appeared unable to bind the Qa-SNARE in binary complex, much as was deduced previously from in vitro pull-down assays with the soluble Qa-SNARE protein (Karnik et al., 2013b).

To test its effect on secYFP traffic, we used the pTecG-2in1-CC vector to express SEC11^{L128R} without and with SYP121$^{\Delta C}$ in wild-type, *syp121*, and *syp122* Arabidopsis. Figure 7 includes one set of fluorescence images, and the analysis of all transformations includes data from the parallel control and assays with SYP121$^{\Delta C}$ (Figures 2 to 5). Comparison of the fluorescence images and ratios shows that SEC11^{L128R} was without significant effect on YFP retention when expressed on its own in wild-type and *syp121* mutant plants. However, expressing SEC11^{L128R} alone in the *syp122* mutant led to secYFP retention and a high mean fluorescence ratio, similar to that observed in seedlings expressing the SYP121$^{\Delta C}$ fragment. Furthermore, SEC11^{L128R} expression was ineffective in preventing secYFP retention, both in wild-type Arabidopsis and in the mutant lines coexpressing SYP121$^{\Delta C}$. Thus, contrary to our expectation, the results suggested not only that association with the native SYP121 N terminus is important for SEC11 rescue of traffic but that SEC11^{L128R} itself suppresses secretory traffic when SYP121 provides the dominant pathway for secretion at the plasma membrane.

The SEC11$^{\Delta 149}$ Peptide Blocks SYP121-Mediated Secretory Traffic

Proteins of the SM family are characterized by common structural elements (Misura et al., 2000; Südhof and Rothman, 2009; Hu et al., 2011; Rizo and Südhof, 2012), including an N-terminal domain (so-called domain 1) and two additional domains, the last of these divided by a "hinge" that forms the apex of the clothespeg-like structure (Figure 8A). Studies of neuronal nSec1 in complex with the Qa-SNARE Syn1A have implicated domain 1 (residues 4 to 134 of nSec1) in binding with the closed conformation of the Qa-SNARE to sequester it in a fusion-incompetent state (Südhof and Rothman, 2009). Similar associations may also occur in yeast (Furgason et al., 2009) but have yet to be explored in plants. Following alignments with nSec1 and its homolog Munc18-1 (Figure 8B), we designed constructs to express a domain 1 peptide spanning residues 1 to 149 of SEC11 (SEC11$^{\Delta 149}$) without and with the mutation of residue Leu-128 (SEC11$^{\Delta 149,L128R}$). We also designed a construct to express a second peptide corresponding to domain 2 spanning residues 150 to 270 (SEC11$^{\Delta 150\text{-}270}$).

To test if SYP121 binds SEC11$^{\Delta 149}$ in vitro, we used a SYP121$^{\Delta C}$ tagged with streptavidin at its C terminus and the SEC11, SEC11$^{\Delta 149}$, and SEC11$^{\Delta 149,L128R}$ proteins tagged with GST at their N termini, much as described previously (Karnik et al., 2013b). For comparison, we also tested the binding with the cognate SNAREs VAMP721 and SNAP33 (Karnik et al., 2013b). Each of the proteins was expressed in *Escherichia coli* and purified by affinity chromatography prior to assays. Incorporating the tags in this orientation avoided potential interference with the critical domains required for

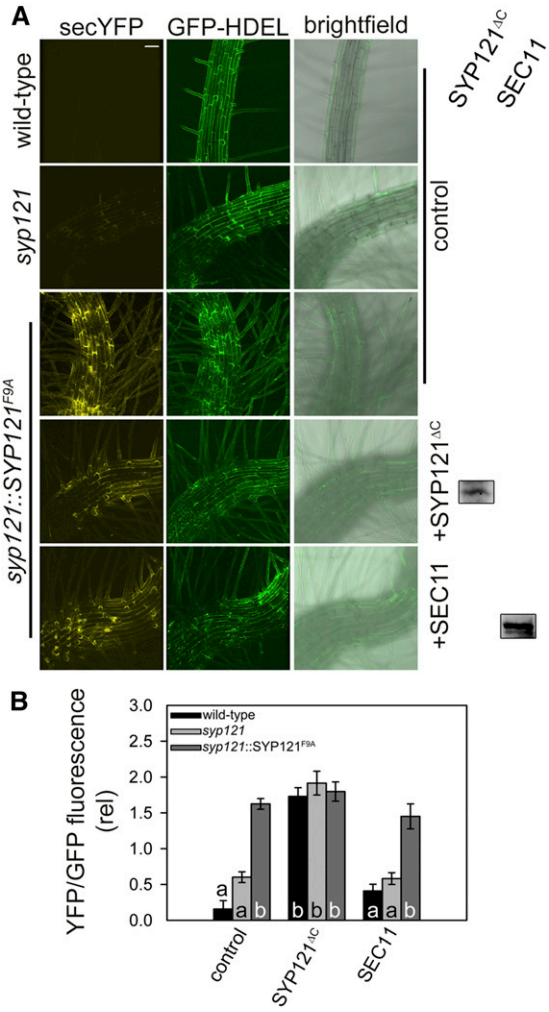

Figure 5. *syp121* Complementation with Full-Length SYP121^{F9A} Alone Is Sufficient to Block Secretory Traffic.

(A) Representative confocal images (left to right) of fluorescence from the secretory marker secYFP and the retained (endoplasmic reticulum) marker GFP-HDEL rendered as 3D projections, along with the corresponding, mid-stack merged bright-field and GFP-HDEL image. Images are of wild-type and *syp121* Arabidopsis seedlings and of *syp121:SYP121^{F9A}* complemented seedlings expressing the full-length mutant SYP121^{F9A} (indicated at left). Each line was transiently transformed to express secYFP and GFP-HDEL with SYP121$^{\Delta C}$ and SEC11 (indicated at right). Immunoblot analysis verifying the expression of SYP121$^{\Delta C}$ and SEC11 using anti-myc and anti-HA antibodies, respectively, is shown at right. Controls with wild-type and *syp121* mutant lines expressing SYP121$^{\Delta C}$ and SEC11 are found in Figures 2 and 3. Bar = 50 μm.

(B) secYFP:GFP-HDEL fluorescence ratios as means ± SE of more than five independent experiments for each construct and Arabidopsis line. Fluorescence ratios were calculated as the mean tissue fluorescence determined from 3D projections of root images after correcting for the background fluorescence similarly recorded from untransformed seedlings of the same age. Significance is indicated by lettering at $P < 0.05$.

protein interactions. The purified protein fusions were used in pull-down assays with affinity resin-bound SYP121$^{\Delta C}$ as the bait and the SM protein and peptides as the prey. The results (Figure 8C) showed that SNAP33, VAMP721, SEC11, and SEC11$^{\Delta 149}$ all bound SYP121$^{\Delta C}$ with signals 4- to 5-fold above background, but SEC11$^{\Delta 149,L128R}$ association with SYP121$^{\Delta C}$ was similar to the background.

To test SEC11 peptide interaction with SYP121 in vivo, we transiently transformed Arabidopsis seedlings using the tricistronic vector pBiFCt-2in1-NC for ratiometric bimolecular fluorescence complementation (rBiFC) (Grefen and Blatt, 2012a; Karnik et al., 2013b; Blatt and Grefen, 2014; Lipka et al., 2014). The 2in1 rBiFC system incorporates a set of independent Gateway-compatible cassettes with coding sequences for the two halves of YFP, nYFP and cYFP, to generate fusion constructs for coexpression and testing of fluorescence complementation in the plant. The vector also includes a third cassette incorporating the coding sequence for a soluble red fluorescent protein (RFP) fluorescent marker that can be used, on a cell-by-cell basis, as a transformation control and ratiometric reference for quantification. Again, to avoid

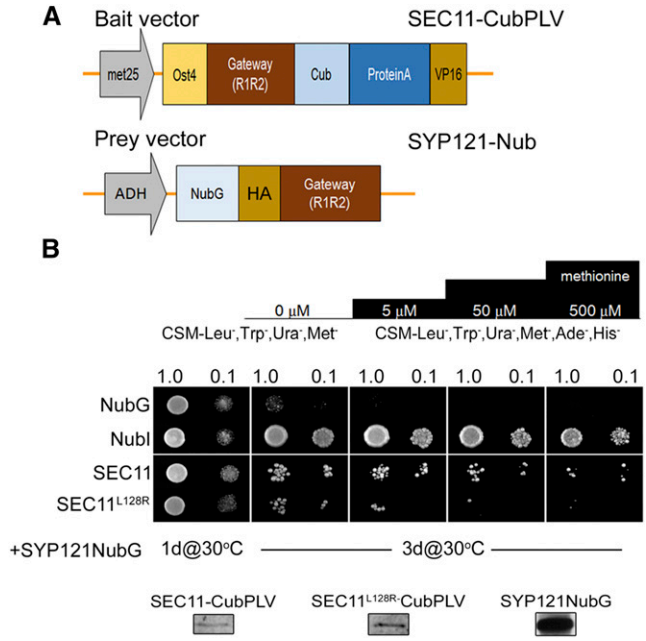

Figure 6. SYP121 Interacts with SEC11 but Not SEC11^{L128R} in a Yeast Mating-Based SUS Assay.

(A) Schematic of the Gateway-compatible vectors used to express bait and prey fusion proteins, including the N-terminal anchor fusion with mOST4.

(B) Yeast mating-based SUS assay using mOST4 fusions of SEC11 and SEC11^{L128R} as baits and SYP121 as the prey along with controls (negative, NubG; positive, NubI). Note that the controls here are for mOST4-SEC11^{L128R} as the bait; controls for mOST4-SEC11 are included in Supplemental Figure 1. Diploid yeast were dropped at 1.0 and 0.1 OD_{600} on CSM medium without Trp, Leu, Ura, and Met to verify mating and on CSM without Trp, Leu, Ura, Met, Ade, and His to test for interaction. Additions of 5, 50, and 500 μM Met were included to suppress bait expression as a test for the specificity of interaction. Immunoblot analysis (5 μg of total protein/lane) of the haploid yeast used for mating is included at bottom using anti-VP16 and anti-HA antibodies to detect prey and bait protein expression, respectively.

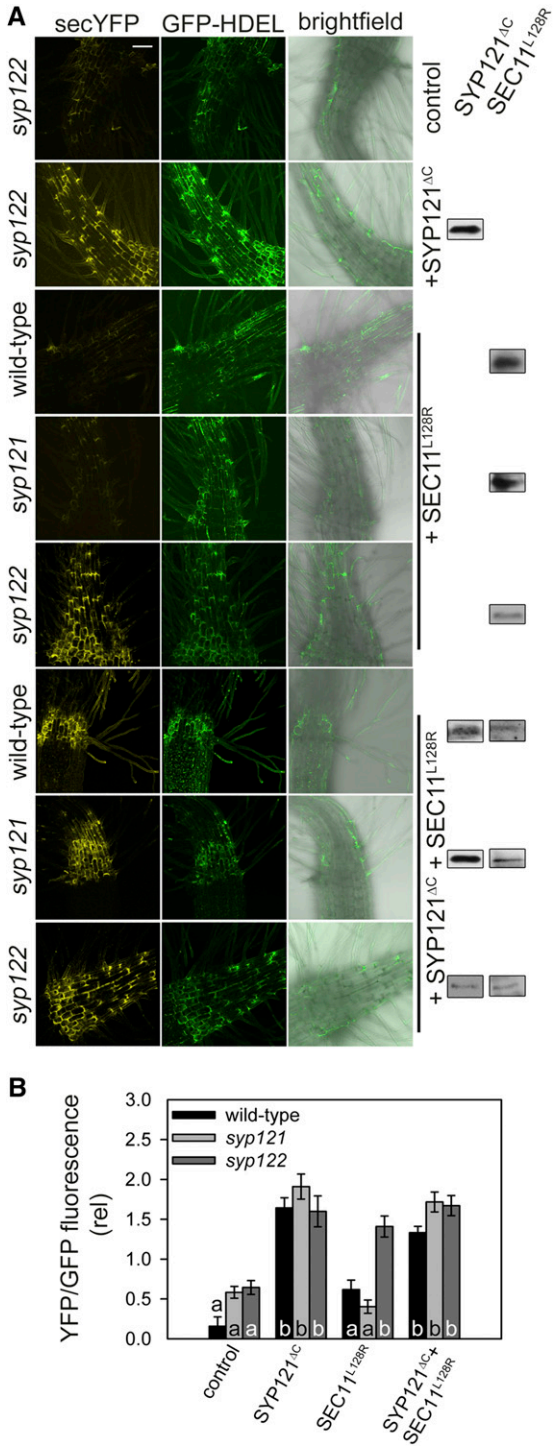

Figure 7. SEC11^{L128R} Blocks Secretion in the *syp122* Mutant.

(A) Representative confocal images (left to right) of fluorescence from the secretory marker secYFP and the retained (endoplasmic reticulum) marker GFP-HDEL rendered as 3D projections, along with the corresponding, mid-stack merged bright-field and GFP-HDEL image. Images are of transiently transformed wild-type, *syp121*, and *syp122* Arabidopsis seedlings (indicated at left) expressing secYFP and GFP-HDEL with SYP121$^{\Delta C}$, SEC11^{L128R}, and SYP121$^{\Delta C}$ + SEC11^{L128R} (indicated at right). Controls for the *syp122* mutant with secYFP and GFP-HDEL alone and with SYP121$^{\Delta C}$ are included for comparison; additional controls are found in Figures 2 and 3. Immunoblot analysis verifying the expression of SYP121$^{\Delta C}$ and SEC11^{L128R} using anti-myc and anti-HA antibodies, respectively, is shown at right. Bar = 50 μm.

(B) secYFP:GFP-HDEL fluorescence ratios as means ± SE of three or more independent experiments for each construct and Arabidopsis line. Fluorescence ratios were calculated as the mean tissue fluorescence determined from 3D projections of root images after correcting for the background fluorescence similarly recorded from untransformed seedlings of the same age. Significance is indicated by lettering at $P < 0.05$.

potential interference of the rBiFC tags, we designed the constructs of SEC11 and its peptides as N-terminal fusions with cYFP, and we used SYP121$^{\Delta C}$ as a C-terminal fusion with nYFP. Figure 8D shows representative confocal images of Arabidopsis expressing SYP121$^{\Delta C}$-nYFP alone as a control and with each of the cYFP-SEC11 fusion constructs. YFP and RFP fluorescence were quantified using the same standardized methods as were applied in the secYFP trafficking assays, and background fluorescence was subtracted before calculating the fluorescence ratios. We found (Figure 8E) that coexpressing SEC11 with SYP121$^{\Delta C}$ led to almost a 5-fold increase in the YFP:RFP fluorescence ratio compared with the background control of SYP121$^{\Delta C}$ expressed alone. Coexpression with SEC11$^{\Delta 149}$ gave a reduced fluorescence ratio roughly 3.5-fold over the control. However, a significant rBiFC signal above the control was not evident on coexpression with SEC11$^{\Delta 149,L128R}$ or on expressing SEC11$^{\Delta 150\text{-}270}$ with SYP121$^{\Delta C}$. These results, and the biochemical data, demonstrate that the SEC11$^{\Delta 149}$ peptide retains the capacity to interact with the Qa-SNARE, and, like full-length SEC11, this association is eliminated by mutation of Leu-128.

We challenged secretory traffic with SEC11$^{\Delta 149}$ in vivo using the pTecG-2in1-CC vector in wild-type, *syp121*, and *syp122* Arabidopsis. Consistent with its capacity for SYP121 binding, expressing SEC11$^{\Delta 149}$ (Figures 9A and 9B) led to a significant increase in secYFP retention, if marginally less than that observed with SYP121$^{\Delta C}$ in the wild-type and *syp122* plants. However, expressing SEC11$^{\Delta 149}$ in the *syp121* mutant failed to promote secYFP retention above the background observed on expressing secYFP and GFP-HDEL alone. To test SEC11$^{\Delta 149}$ binding alternatively to SYP121$^{\Delta C}$ in the *syp121* mutant, we repeated these trials using the SYP122$^{\Delta C}$ and SYP121$^{\Delta C,F9A}$ fragments, neither of which binds SEC11$^{\Delta 149}$, in place of SYP121$^{\Delta C}$ (Supplemental Figures 3 and 4). In this case, SEC11$^{\Delta 149}$ was unable to rescue traffic block by this Qa-SNARE fragment in the *syp121* mutant and, indeed, enhanced block in the wild-type and *syp122* seedlings that carry SYP121. We conclude that SEC11$^{\Delta 149}$ suppresses secretory traffic, analogous to the action of the Qa-SNARE fragment, but in a manner that associates strictly with the presence of the native SYP121 protein. Its rescue of traffic in the *syp121* mutant background is similarly allied to its ability to bind with SYP121$^{\Delta C}$, as we outline in Discussion.

The SEC11$^{\Delta 149}$ Peptide Suppresses Cell Expansion Dependent on SYP121

Finally, we generated independent, stable lines of Arabidopsis in all three genetic backgrounds (wild type, *syp121*, and *syp122*) to

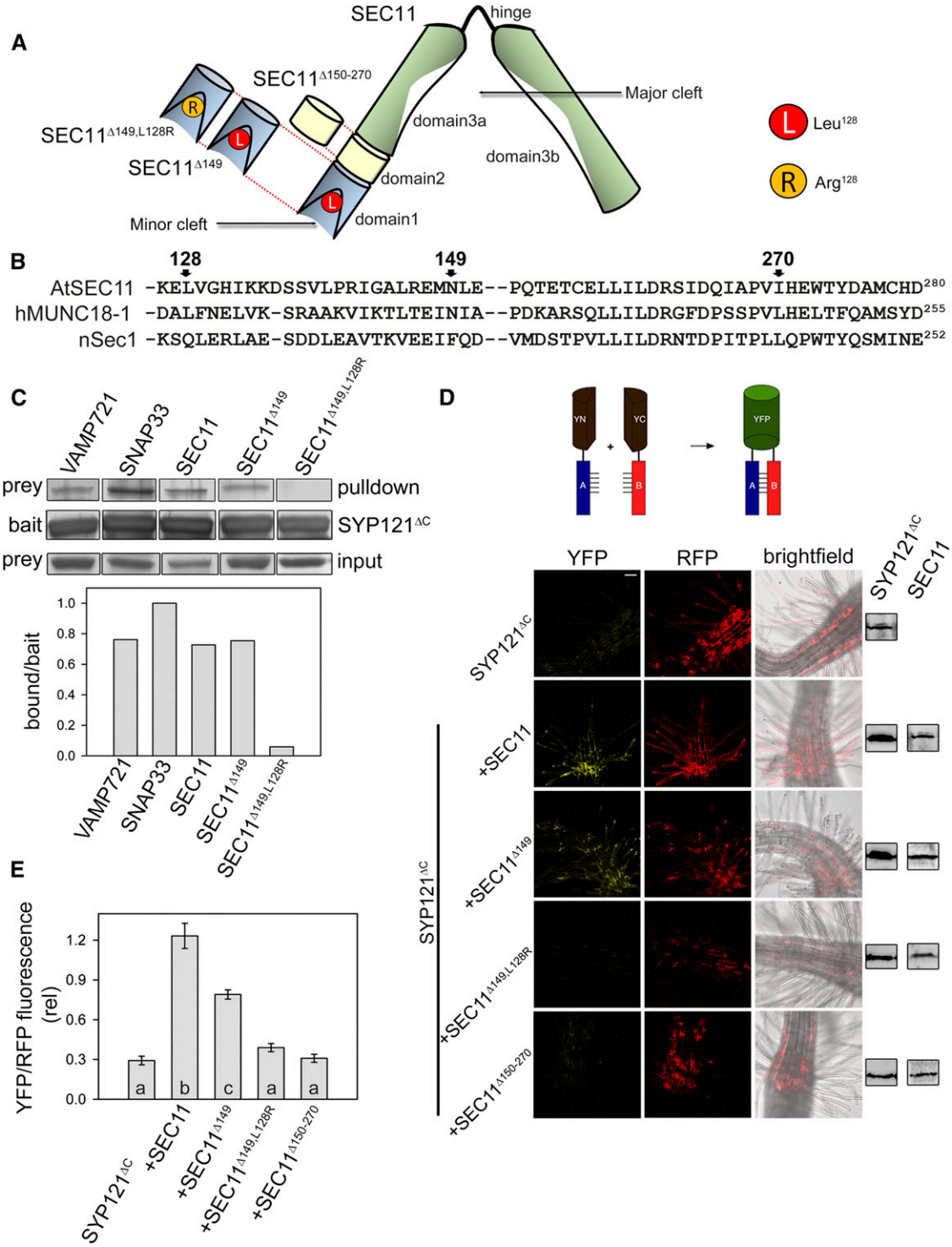

Figure 8. The SEC11$^{\Delta 149}$ Fragment Interacts with SYP121$^{\Delta C}$.

(A) and **(B)** Schematic of SEC11 domain topology, including major and minor clefts as indicated, and alignment with human Munc18-1 and neuronal Sec1 proteins (Misura et al., 2000). Fragments SEC11$^{\Delta 149}$ and SEC11$^{\Delta 150\text{-}270}$, as well as the SEC11$^{\Delta 149,\ L128R}$ mutant, were generated to express as shown. Leu-128 is critical for interaction with the N terminus of SYP121 (Karnik et al., 2013b).

(C) Silver-stained gel images (top) of proteins recovered in pull-down assays with SYP121$^{\Delta C}$-streptavidin as bait. Images of bait and equimolar prey inputs are shown below. Inputs and pull-down bands are GST-tagged preys (left to right) of VAMP721$^{\Delta C}$, SNAP33, SEC11, SEC11$^{\Delta 149}$, and SEC11$^{\Delta 149,L128R}$. Bound:bait ratios are plotted below derived from band intensities recorded using ImageJ (see Methods).

overexpress myc-tagged SEC11$^{\Delta 149}$ under dexamethasone (Dex)-inducible control (Aoyama and Chua, 1997) and to express SEC11-GFP constitutively. Dex induction was found to give maximum expression of the SEC11$^{\Delta 149}$ construct at concentrations above 1 μM and within 12 h of treatment; induction was stable for at least 48 h following a single treatment (Supplemental Figure 5). Plants derived from at least two independent transformed lines for each construct were analyzed for rosette size, fresh and dry weight, leaf number, and leaf development. In the absence of Dex induction, we found no significant differences between the untransformed and transgenic lines carrying the SEC11$^{\Delta 149}$ construct; lines in the *syp121* background showed a marginal reduction in dry weight (Supplemental Figure 6), but the difference was not significant. A small but significant reduction was observed in leaf number in the *syp122* mutant.

Repeated treatments with 10 μM Dex were performed over 3-week periods to induce and maintain transgene expression. We observed a moderate reduction in vegetative growth when SEC11$^{\Delta 149}$ was expressed in the wild-type background compared with the untransformed controls treated with Dex, and a similar, albeit much stronger effect was evident in the *syp122* mutant background; by contrast, no differences in rosette size and fresh or dry weight were recovered with SEC11$^{\Delta 149}$ expression in the *syp121* background, although immunoblot analysis confirmed expression of the transgene in each case (Figures 10A to 10D). Plants expressing SEC11$^{\Delta 149}$ in the wild-type and *syp122* backgrounds yielded fewer leaves that were generally smaller (Figures 10D and 10E). We also analyzed the growth of lines constitutively expressing SEC11-GFP in the same genetic backgrounds. Vegetative growth and fresh and dry weights in this case were enhanced for all independent lines in the wild-type and *syp122* backgrounds but not in the *syp121* mutant background. This effect was most evident 3 to 4 weeks after germination (Figure 11); however, differences in rosette area and biomass were not significant 5 to 6 weeks after the onset of flowering, suggesting that SEC11 overexpression accelerated growth only early on prior to floral induction.

Because the epidermal layer of the leaf is a major determinant of leaf expansion (Walter et al., 2009), we quantified epidermal cell size and numbers in fully expanded leaves of untransformed plants and plants expressing the Dex-inducible SEC11$^{\Delta 149}$ construct, both after 3-week treatments with Dex. We found the *syp122* mutant and to a lesser extent the wild-type backgrounds to show smaller mean epidermal cell areas when compared with their corresponding controls without Dex (Figures 12A and 12B). All of the lines developed a primary inflorescence after 5 to 6 weeks. In the *syp122* background especially, SEC11$^{\Delta 149}$ expression was associated with curling of the leaf edges and reduced inflorescence size (Figures 12C and 12D). Even after 8 weeks, these plants showed a smaller inflorescence compared with the other controls and transgenic lines. Although separating the developmental sequence in heterogeneous tissues is not straightforward, overall the observations suggest that SEC11$^{\Delta 149}$ expression affects primarily cell expansion rather than cell division. Most significant, however, the SEC11$^{\Delta 149}$ phenotype associated with the presence of the native SYP121 in the parental background and showed a dominance even in the wild-type background, much as we found for secYFP retention. These observations point to a crucial role for the SEC11 and its N-terminal domain in regulating traffic to the plasma membrane, and they underline the specific association of the SM protein with SYP121.

DISCUSSION

The Arabidopsis Qa-SNAREs SYP121 (=SYR1/PEN1) and SYP122 exhibit high sequence homology and overlapping functions, and both are present at the plasma membrane of cells throughout the plant (Lipka et al., 2007; Bassham and Blatt, 2008). Along with the Qa-SNARE SYP132, which is constitutively expressed and present at low levels (Enami et al., 2009), these proteins mediate secretory vesicle traffic, contributing to cellular homeostasis, expansion, and growth (Blatt, 2000; Shope et al., 2003; Campanoni and Blatt, 2007). Functional differences between SYP121 and SYP122 are known (Leyman et al., 1999; Zhang et al., 2007; Rehman et al., 2008; Honsbein et al., 2009, 2011; Grefen et al., 2010a; Eisenach et al., 2012), but as these Qa-SNAREs share cognate partners (Kwon et al., 2008; Karnik et al., 2013b; Yun et al., 2013), studies to date have offered few clues to the mechanistic basis for the differences in their regulation and function. Among other factors, SM proteins are widely recognized to be key components that regulate SNARE-mediated vesicle traffic, both in stabilizing the cognate SNARE complex and in controlling the availability of several Qa-SNAREs for binding (Südhof and Rothman, 2009; Rizo and Südhof, 2012). Arabidopsis harbors six SM proteins, including SEC11, which was identified originally with another Qa-SNARE, SYP111, in membrane traffic during cell division (Waizenegger et al., 2000; Assaad et al., 2001; Park et al., 2012). Only recently was SEC11 shown to bind with SYP121 and affect traffic at the plasma membrane mediated by this Qa-SNARE (Karnik et al., 2013b).

We have examined the specificity of SEC11, taking advantage of the soluble domains of the Qa-SNAREs, SYP121$^{\Delta C}$ and SYP122$^{\Delta C}$, that act as dominant-negative (inhibitory) fragments and block secretory traffic (Geelen et al., 2002; Tyrrell et al.,

Figure 8. (continued).

(D) rBiFC images collected from Arabidopsis seedlings transiently transformed to express SYP121$^{\Delta C}$ and each of the SEC11 fragments fused to cYFP and nYFP, respectively. Images are rendered as 3D projections corresponding (left to right) to the YFP (rBiFC) and soluble RFP fluorescence signals. The corresponding mid-stack bright-field plane is included at right. Constructs with the SYP121$^{\Delta C}$-cYFP fusion alone were included as an additional control. Immunoblot analysis to verify the expression of the fusion proteins is shown at far right. Bar = 50 μm.

(E) Means ± SE of fluorescence ratios (YFP:RFP) were calculated from the mean fluorescence intensities determined from 3D projections of root images from five or more seedlings after correcting for background recorded from untransformed seedlings. Significance of differences is indicated by letters ($P < 0.01$).

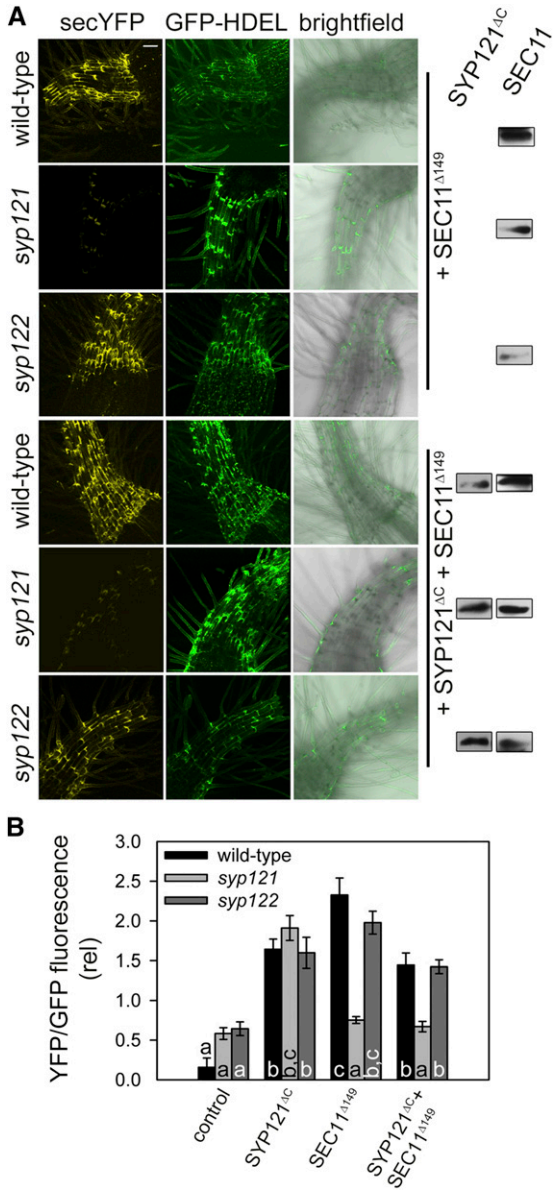

Figure 9. The SEC11$^{\Delta 149}$ Fragment Blocks Secretory Traffic, but Only in the Presence of the Native SYP121.

(A) Representative confocal images (left to right) of fluorescence from the secretory marker secYFP and the retained (endoplasmic reticulum) marker GFP-HDEL rendered as 3D projections, along with the corresponding, mid-stack merged bright-field and GFP-HDEL image. Images are of transiently transformed wild-type, *syp121*, and *syp122* Arabidopsis seedlings (indicated at left) expressing secYFP and GFP-HDEL together with SEC11$^{\Delta 149}$ alone and together with SYP121$^{\Delta C}$ (indicated at right). Immunoblot analysis verifying the expression of the Qa-SNARE and SEC11$^{\Delta 149}$ fragments using anti-myc and anti-HA antibodies is shown at right. Bar = 50 μm.

(B) secYFP:GFP-HDEL fluorescence ratios as means ± SE of more than eight independent experiments for each construct and Arabidopsis line. Fluorescence ratios were calculated as the mean tissue fluorescence determined from 3D projections of root images after correcting for the background fluorescence similarly recorded from untransformed seedlings of the same age. Significance is indicated by lettering at $P < 0.05$.

2007), and of the *syp121* and *syp122* mutant Arabidopsis. These studies led to a substantial reassessment of roles for the SM protein. Most important, the findings establish a function for SEC11 in selective regulation of SYP121-mediated traffic at the plasma membrane. They offer strong evidence that the SYP121$^{\Delta C}$ and SYP122$^{\Delta C}$ fragments block traffic by sequestering the cognate SNARE partners, thereby competing for their binding with the full-length Qa-SNAREs at the plasma membrane. They indicate that SEC11 interaction with the SYP121 N terminus is crucial in preparing the Qa-SNARE for vesicle fusion. Finally, they suggest that binding of SEC11 to the SYP121 N terminus has an unexpected and complementary role in "unlocking" the SNARE complex for its recycling following vesicle fusion.

SEC11 Is Selective among Plasma Membrane Qa-SNAREs

Previous studies had indicated a lack of specificity among soluble fragments of the plasma membrane SNAREs to mediate the block of secretion. Tyrrell et al. (2007) noted that the dominant-negative fragments SYP121$^{\Delta C}$ and SYP122$^{\Delta C}$ were almost equally effective in blocking traffic to the plasma membrane, and specificity was evident only between subsets of SNAREs aligned with their target membranes. It was suggested that block by SYP121$^{\Delta C}$ and SYP122$^{\Delta C}$ could be related mechanistically either to competition for a common pool of cognate partners (Misura et al., 2001; Pajonk et al., 2008) or to the ability of the Qa-SNARE fragments to bind with the full-length counterparts quasi-indiscriminately in homomultimers, thereby trapping SYP121 and SYP122, possibly in a semi-crystalline, "closed" conformation (Sieber et al., 2007; Grefen et al., 2011). Our data now provide substantive evidence that the SNARE fragments block traffic by competing for the cognate partners. We found that overexpressing SEC11 rescued secretory traffic independent of the dominant-negative SNARE fragment, but only in the background of Arabidopsis expressing the native SYP121 at the plasma membrane (Figure 3). The requirement for the native SYP121, especially, militates against the argument for SEC11 overexpression simply titrating out the SYP121$^{\Delta C}$ fragments, and the observations are equally difficult to explain if SYP121$^{\Delta C}$ and SYP122$^{\Delta C}$ assembled indiscriminately with the full-length Qa-SNARE proteins. Instead, the results are most easily understood if SEC11 rescue arose from its stabilization of the SNARE core complex with SYP121, thereby accelerating traffic and outcompeting SYP121$^{\Delta C}$ block. Significantly, the block of traffic was also seen on overexpressing the SYP121$^{\Delta C,F9A}$ mutant (Supplemental Figure 2), and its effect, likewise, was rescued by coexpressing SEC11 in wild-type Arabidopsis (Figure 4). Because the SYP121$^{\Delta C,F9A}$ mutant on its own does not bind with SEC11 (Karnik et al., 2013b), the observations preclude a titration of the soluble Qa-SNARE fragments and lead to the conclusion that these fragments must block traffic by sequestering the cognate SNAREs in complexes that are unable to complete the fusion process.

These experiments also yield insights into the specificity of SEC11 in regulating secretory traffic. Both SYP121 and SYP122 are able to mediate traffic at the plasma membrane, and soluble fragments of both the SNAREs were found to block secretory traffic in wild-type or *syp121* and *syp122* Arabidopsis (Figure 2).

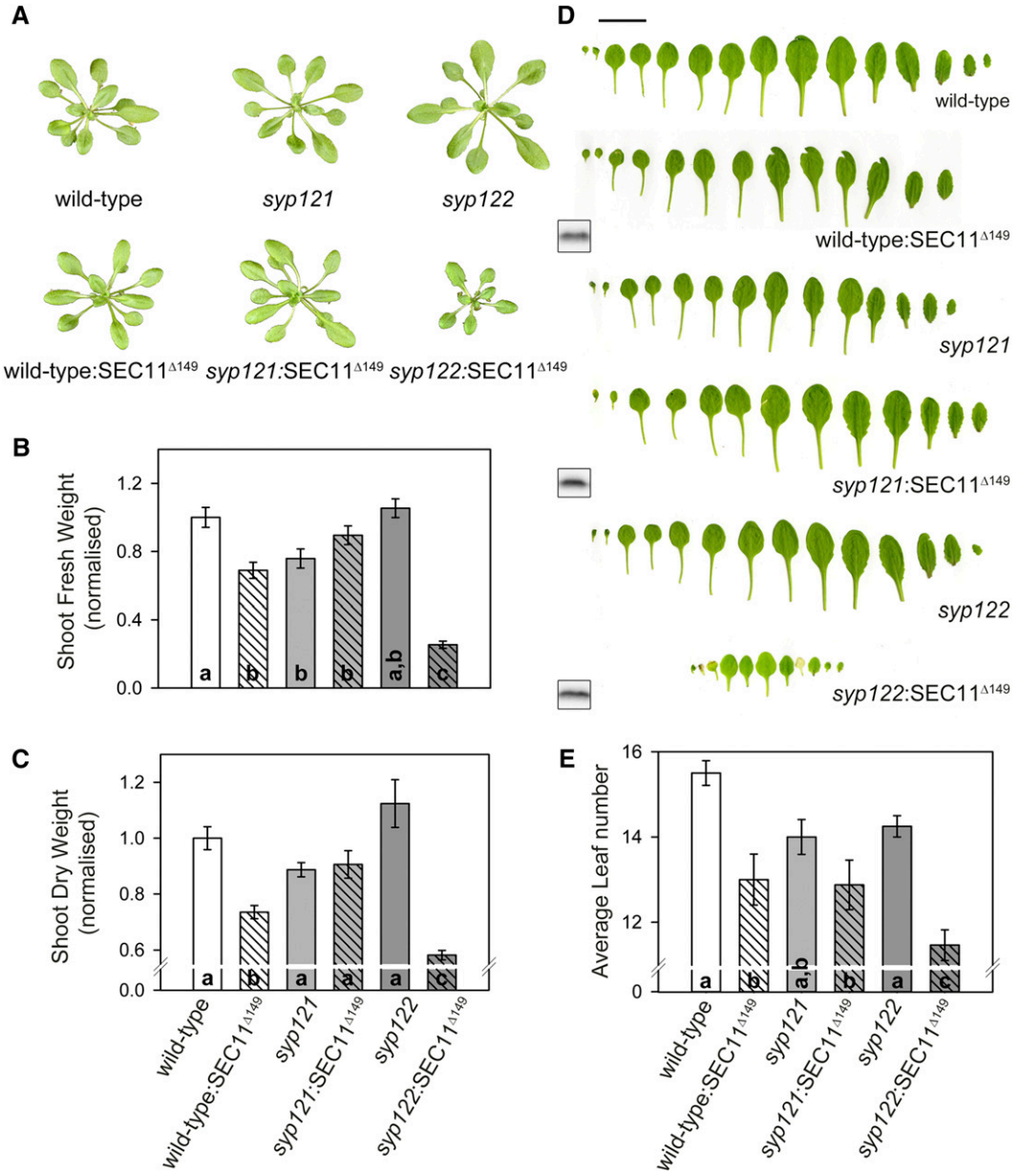

Figure 10. SEC11$^{\Delta 149}$ Expression Affects Growth in Wild-Type and *syp122*, but Not in *syp121*, Arabidopsis.

(A) Three-week-old Arabidopsis expressing SEC11$^{\Delta 149}$ under the control of the Dex-inducible promoter in the wild-type, *syp121*, and *syp122* backgrounds. Images are of plants treated daily with 10 μM Dex beginning 7 d after germination.

(B) and **(C)** Mean ± SE for shoot fresh and dry weights from the wild-type and mutant backgrounds and three independently transformed lines each, comprising >50 plants per line. Values are normalized to the untransformed wild type, and significance is indicated by letters ($P < 0.05$).

(D) Developmental progression of leaves from representative plants as in **(A)**. Immunoblots using anti-myc antibodies for expression of the Dex-induced construct in each case are included. Bar = 1 cm.

(E) Mean ± SE of leaf numbers from >50 plants as in **(A)** to **(C)** with significance indicated by letters ($P < 0.05$).

It is significant, therefore, that SEC11 rescued secretory traffic, but only so long as the native SYP121 was present (i.e., in wild-type and *syp122* Arabidopsis) but not in the *syp121* mutant, where only native SYP122 was present (Figure 3). Experiments with the N-terminal domain of SEC11 complement these findings, and we will return to this point shortly. Of course, SEC11 is known also to bind with SYP111 (=KNOLLE), a homolog of SYP121 and SYP122 (Assaad et al., 2001). However, SYP111 is expressed only during cytokinesis (Lauber et al., 1997), and it does not overlap functionally with SYP121 (Muller et al., 2003; Reichardt et al., 2011). Indeed, the association with SYP121, and the actions of SEC11 and SEC11$^{\Delta 149}$ when stably

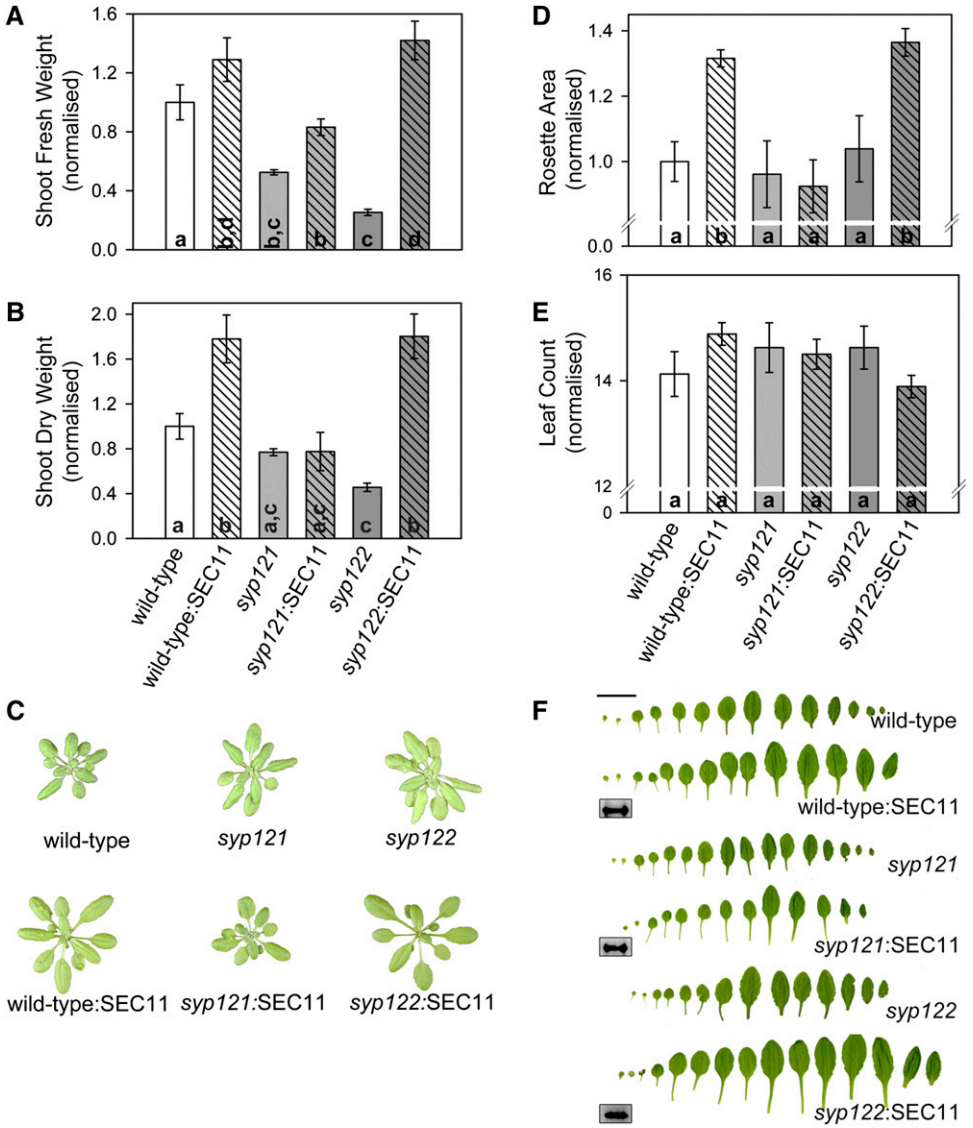

Figure 11. SEC11 Overexpression Enhances Early Vegetative Growth in Wild-Type and *syp122*, but Not in *syp121*, Arabidopsis.

(A), **(B)**, **(D)**, and **(E)** Mean ± SE for rosette area, shoot fresh and dry weights, and leaf counts (see **[F]**) from the wild-type and mutant backgrounds and three independently transformed lines each, comprising >50 plants per line. Values in **(A)** and **(D)** are normalized to the untransformed wild type, and significance is indicated by letters ($P < 0.05$).

(C) Three-week-old Arabidopsis constitutively overexpressing SEC11 in the wild-type, *syp121*, and *syp122* backgrounds.

(F) Developmental progression of leaves from representative plants as in **(A)**. Immunoblots using anti-myc antibodies for expression of the SEC11 construct in each case are included. Bar = 1 cm.

overexpressed, also raise questions about whether the effects of the *sec11* (=*keule*) null mutation are solely the result of its impairing cell division (Assaad et al., 2001). Resolving the molecular determinants of SEC11 specificity for SYP111 and SYP121 now presents technical challenges. Like K^+ channel specificity for SYP121 (Grefen et al., 2010a), SEC11 binding to the SYP121 N terminus almost certainly depends on residues adjacent to the highly conserved Phe-9 of the Qa-SNARE, but its resolution will require dissecting binding between two distinct sites of the SM protein and two different locations on the SNARE (Karnik et al., 2013b). Regardless, however, SEC11 action is clearly selective for SYP121 at the plasma membrane.

SYP121 and SEC11 N Termini Mediate in Traffic Control at the Plasma Membrane

Binding of SEC11 to SYP121 exhibits two distinct modes that roughly parallel those described for SM proteins in mammals and yeast (Dulubova et al., 2007; Südhof and Rothman, 2009) and associate with two binding sites on the SM protein (Karnik

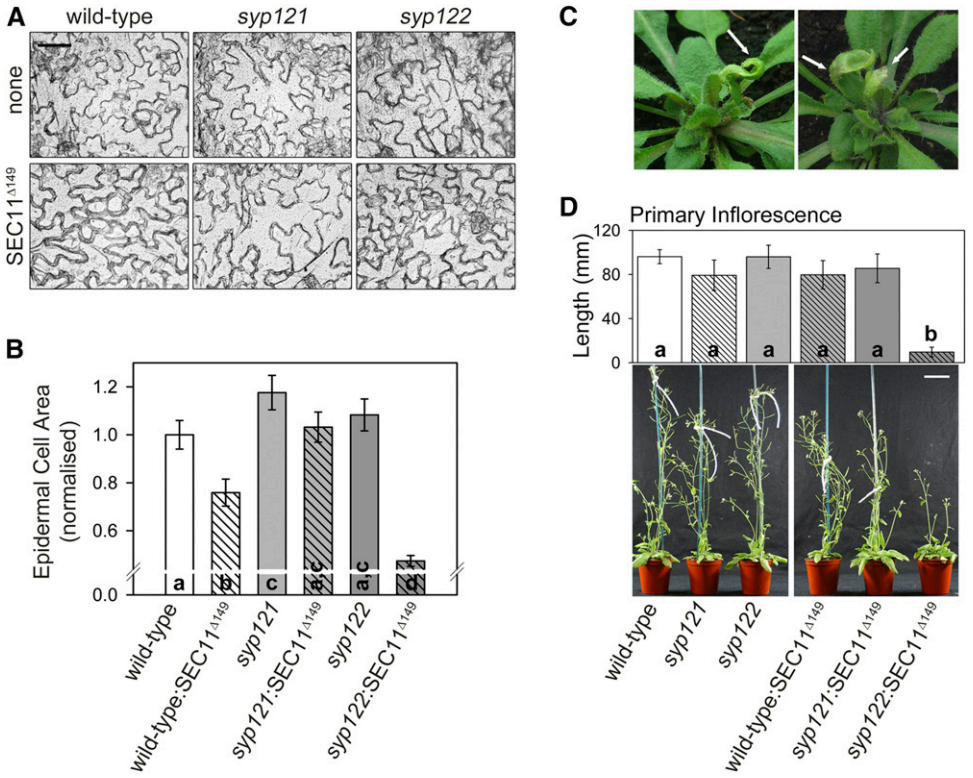

Figure 12. SEC11$^{\Delta149}$ Expression Affects Epidermal Cell Size and Inflorescence Development.

(A) Epidermis of fully expanded leaves from 3-week-old Arabidopsis expressing SEC11$^{\Delta149}$ under the control of the Dex-inducible promoter in the wild-type, *syp121*, and *syp122* backgrounds. Images are from plants treated as in Figure 10 and were acquired at 40× objective magnification. Bar = 20 μm.
(B) Mean ± SE for epidermal cell size from the wild-type and mutant backgrounds and three independently transformed lines each, comprising >5 plants per line and >40 images taken randomly from leaf numbers 6 to 8 of each plant. Values are normalized to the untransformed wild type, and significance is indicated by letters ($P < 0.05$).
(C) Closeup images showing aberrant and necrotic leaves (arrows) formed in lines expressing SEC11$^{\Delta149}$ in the *syp122* mutant background.
(D) Images and mean ± SE for inflorescence length of the lines in **(A)** after 8 weeks of growth. Statistical differences are indicated by letters ($P < 0.01$). Bar = 5 cm.

et al., 2013b). In contrast with its mammalian and yeast counterparts, however, SEC11 binding to the N terminus of SYP121 is competitive with that of VAMP721 and SNAP33, and it has been associated with a stable, quasi-open conformation of the Qa-SNARE that is unable to assemble with these cognate partners (Karnik et al., 2013b). Our findings here complement these observations with a similar divergence in the effects of the SM protein in vivo. Whereas in mammals, overexpressing Munc18-1 promotes traffic block by the cytosolic domain of the Qa-SNARE Syn1A (Khvotchev et al., 2007), we observed SEC11 overexpression to rescue traffic blocked by the SYP121$^{\Delta C}$ fragment, and in a manner dependent on the native SYP121 (Figure 3). Not only do these findings underscore the specificity of SEC11 binding, but they point to a mass-action effect to promote traffic through binding with the native Qa-SNARE.

Bimolecular interactions of SEC11 are suppressed with SYP121^{F9A} (Karnik et al., 2013b). Thus, the *syp121:SYP121^{F9A}* complementation provided an important test of the requirement for binding with the SYP121 N terminus. Since SEC11 was expected to bind SYP121^{F9A} only in complex, we reasoned that the complementation might counter traffic block by SYP121$^{\Delta C}$ by enhancing the stability of SYP121 in the SNARE complex. Instead, we found that secretory traffic was suppressed in plants expressing SYP121^{F9A} and that traffic was not recovered by overexpressing SEC11 (Figure 5). We also tested secretory traffic with the mutant SM protein SEC11^{L128R}. This mutant retains the ability to bind in complex with SYP121, VAMP721, and SNAP33, but its interaction with the Qa-SNARE N terminus is virtually lost in binary complex (Figure 6) (Karnik et al., 2013b). Expressing the SEC11^{L128R} mutant in vivo also suppressed secretory traffic independent of SYP121$^{\Delta C}$, but in this case, the effect was evident only in the *syp122* background; in other words, only if SYP121 was the principal Qa-SNARE at the plasma membrane (Figure 7).

How might these several observations be reconciled? We can start from the premise that SEC11 binding is selective for SYP121 (Figures 2 to 4; Supplemental Figures 1 and 2). Keep in mind that the studies were performed against the background of native SEC11 and, for the SYP121^{F9A}-complemented plants, of SYP122 expression. Therefore, SEC11^{L128R} will have competed with the native SEC11 to block traffic, but only when SYP121 dominated secretion, whereas the exchange of SYP121^{F9A} for SYP121 eliminated all binding of the Qa-SNARE N terminus with

SEC11. Note, too, that SEC11 binding is associated both early in the SNARE cycle with the closed and quasi-open conformations of SYP121 and also late in the SNARE cycle with SYP121 in the SNARE complex (Karnik et al., 2013b). One simple explanation aligns with these two binding modes: it postulates that SEC11 binding to the N terminus of SYP121 is essential for "levering" the SM protein from SYP121 in the quasi-open conformation early in the SNARE cycle and is equally important for discharging SEC11 from SYP121 and the SNARE complex late in the cycle. This explanation is compatible with the binding characteristics of SEC11, SEC11^{L128R}, and especially with the weaker effect of the SYP121^{F9A} mutant in bimolecular interaction with SEC11 (Karnik et al., 2013b). It predicts that the SYP121^{F9A} complementation, like SYP121$^{\Delta C,F9A}$ expression (Supplemental Figure 2), suppresses SYP121- and SYP122-mediated traffic, because it sequesters the cognate SNAREs that are shared between these pathways. In other words, by preventing SEC11 binding to the N terminus at a late stage in the cycle, the cognate SNAREs become trapped in complex with SYP121 and SEC11. Of course, exit from the quasi-open conformation with SEC11 may also be suppressed on complementing the *syp121* mutant with SYP121^{F9A}, but this action cannot explain a block of traffic via SYP122.

By contrast, because SEC11^{L128R} must compete with the native SEC11, its efficacy in block will be diluted, especially when traffic can also pass through the SYP122 pathway (Figure 7). This explanation accords with present models for SM interactions with several Qa-SNAREs (Rathore et al., 2010; Rizo and Südhof, 2012; Archbold et al., 2014). It is consistent, too, with recent studies of the yeast and mammalian SM proteins Sly1p (Demircioglu et al., 2014) and Munc18-1 (Christie et al., 2012), which appear to bind their cognate Qa-SNAREs concurrently via the major cleft and the N-terminal site on the SM protein. In the case of Sly1p, binding to the N-terminal site has been suggested to be important for forming a quasi-open or "loosened" conformation of the Qa-SNARE. In effect, binding between the N termini of Sly1p and its cognate Qa-SNARE Sed5p may create a molecular fulcrum that helps in prising open the Qa-SNARE prior to SNARE complex assembly. Most important, this explanation complements the prediction (above) that SEC11 binding to the SYP121 N terminus is important for SEC11 discharge from the SYP121-SNARE complex and complex disassembly after vesicle fusion. In fact, almost nothing is known of SM protein debinding from the SNARE complex in any eukaryotic system. This explanation is the simplest that accounts for all of our observations, and it should now stimulate thinking about roles for SM proteins in the final stages of SNARE complex recycling.

The SEC11 N Terminus Suppresses Cell Expansion and Vegetative Growth

One of the most intriguing discoveries we present is that expressing the SEC11$^{\Delta 149}$ fragment on its own was sufficient to block vesicle traffic and to suppress vegetative growth (Figures 9, 10, and 12). In this respect, the action of SEC11$^{\Delta 149}$ is similar to that of the *syp121:SYP121^{F9A}* complementation. Like the complementation, SEC11$^{\Delta 149}$ block dominated secretory traffic even in wild-type Arabidopsis that maintains both SYP121- and SYP122-mediated pathways (Figure 5). This pattern of block is a close counterpoint to SEC11 rescue from secretory block by the SYP121$^{\Delta C}$ and SYP122$^{\Delta C}$ fragments (Figure 3). SEC11$^{\Delta 149}$ incorporates determinants of interaction with the N terminus of SYP121, and it retains the ability to bind with SYP121 in vitro and in vivo (Figure 8). However, it lacks the C-terminal half of SEC11 that is essential to form the major SM binding cleft (Rizo and Südhof, 2012; Karnik et al., 2013b; Archbold et al., 2014). So a straightforward interpretation of its functional activity is that SEC11$^{\Delta 149}$ must bind with SYP121 at the plasma membrane, competing with the native SEC11 for the Qa-SNARE N terminus. Furthermore, this binding also must occur late in the SNARE cycle in order to suppress disassembly of the SNARE complex and sequester the cognate SNARE proteins. As with the *syp121:SYP121^{F9A}* results, this prediction is the simplest that explains the dominance of SEC11$^{\Delta 149}$ block when expressed on its own in wild-type Arabidopsis that maintains the SYP122-dependent pathway: SEC11$^{\Delta 149}$ may also bind in binary complex with SYP121, but such binding cannot explain its action in blocking traffic in the wild-type plants. The prediction also provides a plausible explanation for traffic rescue in the *syp121* mutant when coexpressed with SYP121$^{\Delta C}$ (Figure 9). In the latter case, the Qa-SNARE fragment will have been the only ligand available for SEC11$^{\Delta 149}$, and its binding can be understood to sequester SYP121$^{\Delta C}$ from interaction with the cognate SNAREs, especially if the latter were enhanced in the absence of the native SYP121. Indeed, this interpretation finds support in our experiments showing that SEC11$^{\Delta 149}$ failed to rescue traffic in the *syp121* mutant background when coexpressed with SYP122$^{\Delta C}$ and SYP121$^{\Delta C,F9A}$ (Supplemental Figures 3 and 4). Since the SM protein does not bind either (Supplemental Figure 1) (Karnik et al., 2013b), its fragment will not have sequestered the Qa-SNARE fragment and therefore failed to rescue traffic in the *syp121* mutant background.

Finally, the characteristics of traffic block by SEC11$^{\Delta 149}$ were mirrored in the growth patterns of stable lines expressing this construct. Following Dex treatment to induce SEC11$^{\Delta 149}$ expression, we observed reduced rosette size, leaf number, and fresh and dry weights in the wild-type and *syp122* backgrounds, but not in the *syp121* mutant background, when compared with the corresponding controls (Figures 10 and 12). Complementary results were observed on stably overexpressing the wild-type SEC11 (Figure 11). In this case, vegetative growth was consistently accelerated in the wild-type and *syp122* backgrounds, and again, no effect on growth was recovered when overexpressing SEC11 in the *syp121* mutant. Translating effects on secretory traffic from the molecular and cellular levels to vegetative growth is inevitably fraught with difficulty. Nonetheless, our analysis indicated that the consequences, notably of traffic block by SEC11$^{\Delta 149}$, were allied to differences in mean cell size, implying an action mediated through the expansion of the tissue rather than through an interference in cell division, such as might have entailed its interaction with SYP111 (Assaad et al., 2001; Sollner et al., 2002). These observations also call into question the earlier premise that the *keule* (*sec11*) mutant phenotype is solely the result of impaired cell division (Assaad et al., 2001).

A Unifying Model for SEC11 Action at the Plasma Membrane

Figure 13 presents a simple model that incorporates all these findings and the background of our knowledge relating to SEC11 and SYP121 in vesicle traffic. SYP121 assembles with the Qbc-SNARE SNAP33 and the R-SNARE VAMP721 (also the nearly identical VAMP722) to form a functional SNARE complex. The

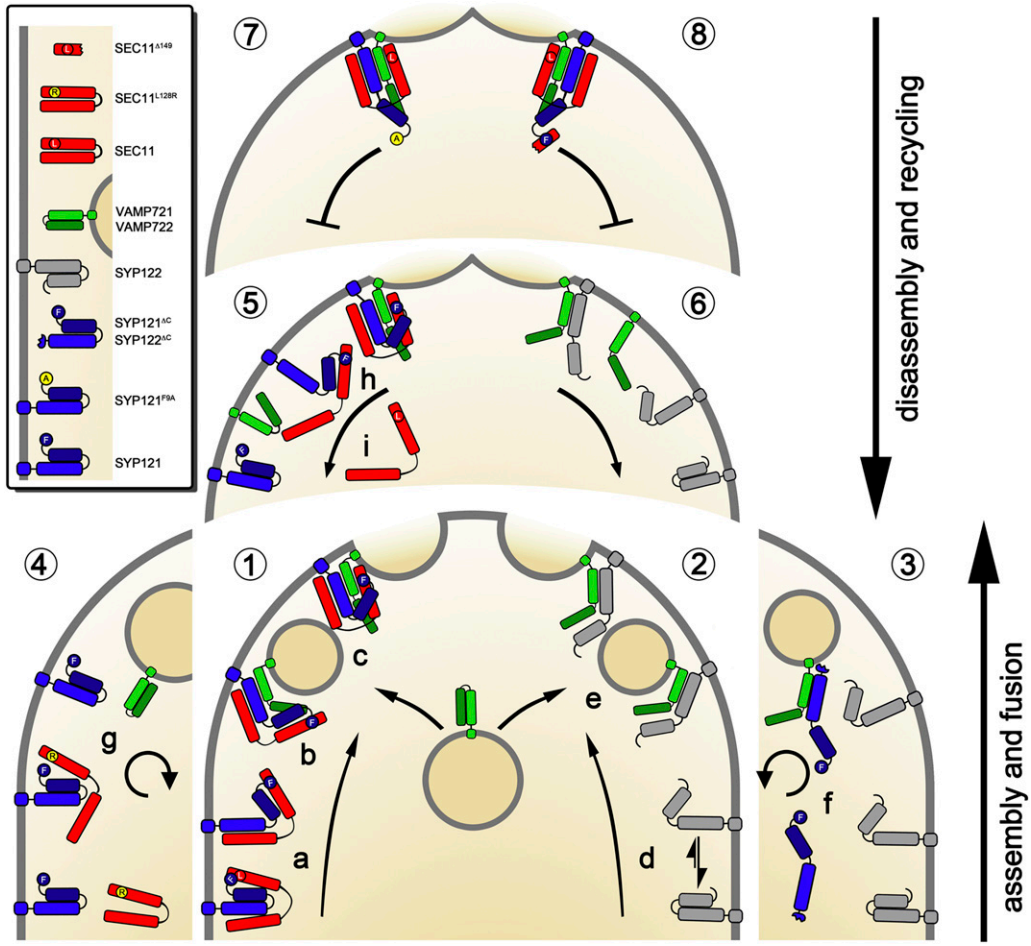

Figure 13. Model of SEC11 Interaction with SYP121 and Its Impact on Secretory Traffic.

Panels 1 to 4 encapsulate the sequence of SNARE assembly, vesicle fusion, and their block by SYP121$^{\Delta C}$, SYP122$^{\Delta C}$, and SEC11^{L128R}. Panels 5 to 8 summarize steps in SNARE complex disassembly and its block by SEC11$^{\Delta 149}$ and SYP121^{F9A}. Additional SNARE components, including SNAP33, are omitted for clarity.

Panel 1. SYP121-mediated traffic is greatly accelerated by binding between Phe-9 of SYP121 and Leu-128 of SEC11, which facilitates opening of the Qa-SNARE (a) and its assembly in complex with cognate SNARE proteins (b). SEC11 then stabilizes the SNARE complex (c) during vesicle fusion.

Panel 2. Traffic proceeds via SYP122 and, to a much lesser extent, via SYP121, independent of SEC11 through opening of the Qa-SNARE (d), which enables SNARE complex assembly (e). Note that SYP121 and SYP122 share a common pool of vesicles as well as the R-SNAREs VAMP721 and VAMP722. Note, too, that SEC11 may bind with SYP121^{F9A} in the SNARE complex, effectively crossing from (e) to (c).

Panel 3. The Qa-SNARE fragments SYP121$^{\Delta C}$ and SYP122$^{\Delta C}$ are able to compete for cognate SNAREs (f), including VAMP721 and VAMP722, thereby preventing the assembly of functional SNARE complexes through both pathways illustrated in panels 1 and 2 and suppressing vesicle fusion at the membrane (here shown only in relation to panel 2).

Panel 4. SEC11^{L128R} is unable to bind and promote SYP121 opening (g). It competes with traffic dependent on SEC11 (panel 1), but not with traffic independent of SEC11 (panel 2), and therefore affects vesicle fusion only when SYP122-dependent traffic is eliminated in the *syp122* mutant.

Panel 5. After vesicle fusion, disassembly of the SYP121 SNARE complex is greatly accelerated through binding between Phe-9 of SYP121 and Leu-128 of SEC11, which facilitates opening of the complex (h) to release SEC11 (i) and, following the action of the NSF ATPase and associated binding factors (omitted for clarity) (Lipka et al., 2007; Bassham and Blatt, 2008), the cognate SNAREs.

Panel 6. Disassembly of SNARE complexes without SEC11 also proceeds through binding with the NSF ATPase and associated binding factors (omitted for clarity) (Lipka et al., 2007; Bassham and Blatt, 2008).

Panel 7. The SNARE complex with SYP121^{F9A} is unable to bind Leu-128 of SEC11, thereby preventing its release and trapping the Qa-SNARE and its cognate partners in complex.

Panel 8. SEC11$^{\Delta 149}$ competes for binding with Phe-9 of SYP121 and thereby prevents the conformational changes required for full-length SEC11 to release the complex. As a consequence, SEC11$^{\Delta 149}$ traps SYP121 and its cognate SNARE partners in complex.

major cleft of SEC11 binds and stabilizes this complex; although not essential for the final stages of vesicle fusion, it greatly accelerates the process. The major cleft of SEC11 also binds SYP121 in the closed conformation. This binary interaction is stabilized by binding between the SYP121 N terminus, which includes Phe-9, and the minor cleft in SEC11 incorporating Leu-128, and it requires the two binding sites of SEC11 to reside on a single polypeptide to lever SYP121 into a quasi-open but fusion-incompetent conformation (Karnik et al., 2013b).

Four conclusions can now be drawn from our observations as outlined above. First, overexpressing SEC11 with SYP121$^{\Delta C}$ rescues traffic, unlike the mammalian model (Khvotchev et al., 2007), and it relies on the native SYP121 (Figure 3). These results imply a mass-action effect through binding with the SNARE complex to promote traffic. Second, we understand the action of SEC^{L128R} (Figure 7) to arise primarily through competition with the wild-type SEC11 for binary association with the major cleft of the SM protein while still permitting the wild-type SEC11 to bind to the SYP121 N terminus. Thus, by binding with two SM polypeptides, it effectively "locks" the closed mode of SYP121 and suppresses traffic when SYP121 is the dominant Qa-SNARE. Third, and by contrast, the SYP121^{F9A} mutant does not compete for SEC11 and must sequester the common pool of cognate SNAREs in order to affect both SYP121- and SYP122-dependent traffic (Figure 5). It follows that SEC11 binding to the SNARE complex, and more importantly its release following assembly and, presumably, vesicle fusion, must be affected by the loss of SEC11 interaction with the SYP121 N terminus. Finally, we interpret traffic block by SEC11$^{\Delta 149}$ to arise similarly through interaction with SYP121 in the SNARE complex. As illustrated, SEC11$^{\Delta 149}$ competes with the bound SEC11 for the SYP121 N terminus and thereby prevents its levering from, and opening of, the SNARE complex. However, it is equally plausible, for example, that SEC11$^{\Delta 149}$ binding to the SNARE complex precludes SEC11 binding as well as locking up the SNAREs in complex. Resolving the detailed mechanics of SEC11 binding that drives SYP121 conformations between the closed, quasi-open, fusion-competent, and SNARE complex forms will now benefit from kinetic and binding affinity analysis. Regardless of the details, our studies lead us to the inevitable conclusion that binding of SEC11 is selective for SYP121 and that its association with the SYP121 N terminus is important not only for the conformational transition of SYP121 to a fusion-competent form but also later for the recycling of SYP121 and its cognate SNAREs from the SNARE complex.

METHODS

Plasmids and Recombinant Proteins

Clones for the expression of tagged recombinant proteins were constructed as described previously (Honsbein et al., 2009; Karnik et al., 2013b). Open reading frames for *SYP121*, *SYP122*, and *SEC11* were amplified with gene-specific primers to include Gateway attachment sites, and primers for mutagenesis were designed using SDM-Assist software (Karnik et al., 2013a) to introduce the desired mutations along with silent mutations that could be used to identify the mutants in restriction digests. Supplemental Table 1 lists the primers used in cloning and site-directed mutagenesis.

Secretion analysis made use of the tetracistronic vector pTecG-2in1-CC (Karnik et al., 2013b), which incorporates four 35S-driven expression cassettes, two carrying the coding sequences for secYFP and for GFP-HDEL. The remaining two cassettes provide Gateway recombination sites (attR3-lacZ-attR2 and attR1-ChloramphenicolR, ccdB-attR4) and a C-terminal tag, either 3xHA or myc (Grefen and Blatt, 2012a). Assays were performed with SEC11 constructs incorporating the C-terminal 3xHA tag and the Qa-SNARE constructs incorporating the C-terminal myc tag (Karnik et al., 2013b). Protein-protein interaction studies in vivo were performed by rBiFC using the tricistronic vector pBiFCt-2in1-NC (Grefen and Blatt, 2012a) with SEC11 constructs nYFP-tagged N terminally and cYFP-tagged SYP121$^{\Delta C}$ tagged C terminally.

SYP121$^{\Delta C}$, SYP122$^{\Delta C}$, and SYP121$^{\Delta C,F9A}$ for pull-down assays were PCR amplified using overlap extension to add 3′ *Nco*I sites, 5′ Flag (DYKDDDDK) tag-StrepII (WSHPQFEK) tag, and *Hin*dIII sites. The genes were introduced into a modified pET28-Duet vector (Invitrogen) for transformation and expression in *Escherichia coli*. Constructs for SUS assays were prepared by cloning the coding sequences for SEC11 and SEC11^{L128R} in the Gateway-compatible pMetOYC-Dest bait vector (below); sequences for SYP121 and SYP122 were cloned in the pNX35-Dest prey vector with a 2xHA tag for verifying expression (Grefen and Blatt, 2012b).

Constructs for stable transformation of *Arabidopsis thaliana* were generated using the Gateway-compatible vectors pDXI-cmyc-Dest and pUBQ10-GFP-Dest (Grefen et al., 2010b) following LR reactions.

pDXIsY-Dest Vector

The RFP expression cassette of the binary vector pBiFC-BB (Grefen and Blatt, 2012a) was replaced by a codon-optimized (Arabidopsis codon usage), gene-synthesized phosphinothricin acetyltransferase (Basta resistance) cassette (flanked by the nos promoter and terminator), yielding vector pBBb. This vector also contains 5′ of the resistance cassette a couple of unique blunt-end restriction sites (*Afe*I, *Pml*I, *Eco*53kI, and *Sna*BI) to facilitate the insertion of other expression cassettes. pDXIsY-Dest was assembled using different gene-synthesized expression cassettes. First, a 35S:GVG-T35S construct was gene synthesized (GVG = GAL4 DNA binding domain, VP16 transactivation domain, glucocorticoid receptor domain) (Aoyama and Chua, 1997) and via blunt-end cloning (*Stu*I) ligated into the *Eco*53kI site in pBBb (see above) to yield pBBb-GVG. This was linearized using *Afe*I, and the gene-synthesized expression cassette 6xUAS-*35S:Gateway:myc-T35S was inserted to create pDXI-Cmyc. This "side product" can be used as a binary Dex-inducible, Gateway-compatible vector. Cutting a 35S:secYFP-T35S construct from pBiFC-BB-secYFP (Karnik et al. 2013b) via *Sma*I/*Sna*BI and inserting it into pDXI-Cmyc via *Sna*BI yielded the final vector pDXIsY-Dest.

SUS and CytoSUS Assays

The CytoSUS vector pMetOYC-Dest was created using a combination of gene synthesis and classical cloning. A fragment of the met25 promoter, starting at the internal *Pml*I site, followed by the 108 bp of OST4p without stop codon and the first 946 bp of the Gateway recombination cassette were gene synthesized (Genscript). This construct as well as pMetYC-Dest (Grefen et al., 2009) were cleaved using restriction endonucleases *Pml*I and *Bss*HII (New England Biolabs), and the gene-synthesized construct was incorporated in the pMetYC-Dest backbone to yield pMetOYC-Dest.

Mating-based SUS assays were performed as described previously (Grefen et al., 2009) using haploid yeast strains, THY.AP4 and THY.AP5, for bait and prey, respectively (Obrdlik et al., 2004; Grefen et al., 2007).

Pull-Down Assays and Immunoblotting

Protein expression was induced in *E. coli* BL21 DE3 cells (Life Technologies) with 1 mM isopropyl β-D-1-thiogalactopyranoside for 4 h, and the proteins were purified by glutathione- and streptactin-coupled Sepharose affinity chromatography and the SYP121$^{\Delta C}$ was immobilized as bait. Pull-downs included GST alone as a background control, and the ratios of proteins

bound to bait were normalized against common standards for comparison as before (Karnik et al., 2013b).

For immunoblot analysis of plant tissues, leaves were excised and flash-frozen in liquid N_2. Frozen tissue was ground in equal volumes (w/v) of homogenization buffer containing 500 mM sucrose, 10% glycerol, 20 mM EDTA, 20 mM EGTA, Protease Inhibitor (Roche), 10 mM ascorbic acid, 5 mM DTT, and 50 mM Tris-HCl, pH 7.4, and centrifuged at 13,000*g* and 4°C for 30 min to pellet debris. Supernatant was diluted 1:1 in 2× Laemmli buffer containing 2.5% 2-mercaptoethanol, heated to 95°C for 10 min, and separated by SDS-PAGE. Proteins from yeast were prepared as described previously (Grefen et al., 2010a). All samples were diluted in loading buffer to 5 μg protein/mL per lane. Ponceau S-stained Rubisco bands were used as loading standards for plant samples. Immunoblots (Karnik et al., 2013b) used primary αSYP121 (1:40,000 dilution), αmyc (1:5000 dilution; Abcam), αHA (1:10,000 dilution; Roche), αSEC11 (1:2000 dilution; Assaad et al., 2001), αGFP (1:10,000 dilution; Abcam), and αVP16 (Roche) antibodies and goat anti-rabbit secondary antibody. Cross-reacting bands were visualized using WestFemto SuperSignal chemiluminescence detection (Thermo Pierce) and imaged by scanning at 1200-dpi resolution. In some experiments, membranes were reprobed after stripping in 100 mM β-mercaptoethanol, 2% SDS, and 62.5 mM Tris-HCl, pH 6.7, at 70°C for 45 min.

Plant Growth, Transformation, and Analysis

Seedlings of Arabidopsis Columbia-0 (wild type) or *syp121-1* (*syp121*) and *syp122-1* (*syp122*) mutants (Honsbein et al., 2009) were transformed transiently as described previously (Grefen et al., 2010b). Stable Arabidopsis lines were generated by floral dip (Clough and Bent, 1998), and transformed seeds were selected by growth on soil with phosphinothricin (Basta; Bayer Cropscience). Homozygous T4 lines were verified for expression of the transgene by immunoblot analysis, and at least two independently transformed lines were chosen for experiments. The *syp121*:*SYP121*^{F9A} complemented line was described previously (Karnik et al., 2013b).

For phenotypic analysis, plants were grown on soil under a 10-h-light/14-h-dark, 18/22°C (light/dark) cycle with 150 μmol m^{-2} s^{-1} PAR. As required, plants were treated at 24-h intervals by spraying with water with and without 10 μM Dex. Rosette size and leaf areas were quantified using ImageJ version 1.48 (imageJ.nih.gov/ij/). Shoot fresh and dry weights were determined after excision and, for dry weights, after drying at 70°C for 3 weeks. Epidermal surface areas were determined with ImageJ from images collected using a Zeiss Axiovert 200 microscope and a Planapo LD40x/0.75NA objective (Zeiss).

Confocal Microscopy

Roots of Arabidopsis seedlings were imaged after 3 to 4 d of cocultivation with *Agrobacterium tumefaciens* using a Zeiss LSM510 META confocal microscope. Images were routinely collected as Z-stacks using Planapo 20x/0.80NA and Planapo 40x/1.3NA (oil) objectives. Excitation intensities, filter settings, and photomultiplier gains were standardized (Tyrrell et al., 2007; Grefen et al., 2010a). For secYFP trafficking studies, GFP and YFP were excited using the 458- and 514-nm lines, respectively, of an Argon2 laser. GFP fluorescence was collected after passage over a 545-nm dichroic mirror and passage through a 475- to 525-nm bandpass filter. YFP fluorescence was collected after passage through a 545-nm dichroic mirror and a 535- to 590-nm bandpass filter. For rBiFC analysis, YFP and RFP were excited by the 514-nm line of an Argon2 laser and the 543-nm line of a HeNe laser, respectively. YFP fluorescence was collected after passage through a 515-nm dichroic mirror and a 535- to 590-nm bandpass filter. RFP fluorescence was collected after passage through a 560-nm dichroic mirror and a 560- to 615-nm bandpass filter. Fluorescence images were rendered as 3D projections, and fluorescence intensities were quantified from the roots after subtracting the mean background fluorescence collected from similarly rendered projections of untransformed seedlings grown in parallel in each case.

Statistical Analysis

All data are reported as means ± SE of *n* independent measurements. Statistical analysis was performed using Sigmaplot 11.2 (Systat, SPSS). Significance was determined using the Holm-Sidak test and ANOVA.

Accession Numbers

Sequence data from this article can be found in the Arabidopsis Genome Initiative or GenBank/EMBL databases under the following accession numbers: SYP121 (At3g11820), SEC11 (At1g12360), VAMP721 (At1G04750), and SNAP33 (At5G01010).

Supplemental Data

Supplemental Figure 1. SEC11 Interacts Selectively with SYP121 over SYP122.

Supplemental Figure 2. Phe^{9} of SYP121$^{\Delta C}$ Is Not Essential for Secretory Block.

Supplemental Figure 3. The SEC11$^{\Delta 149}$ Fragment Fails to Rescue Secretory Traffic Block by SYP122$^{\Delta C}$ in the *syp121* Mutant.

Supplemental Figure 4. The SEC11$^{\Delta 149}$ Fragment Fails to Rescue Secretory Traffic Block by SYP121$^{\Delta C,F9A}$ in the *syp121* Mutant.

Supplemental Figure 5. Time-Course and Dexamethasone Concentration Dependence of SEC11$^{\Delta 149}$ Expression.

Supplemental Figure 6. Normal Growth of Lines Carrying the Dexamethasone-Inducible SEC11$^{\Delta 149}$ Construct.

Supplemental Table 1. Primer Sequences Used for Cloning SYP121$^{\Delta C}$, SYP122$^{\Delta C}$, SEC11, SEC11$^{\Delta 149}$, VAMP721, and SNAP33, for Site-Directed Mutagenesis of SEC11 and SYP121, and PCR for StrepII-Tagged SYP121$^{\Delta C}$.

ACKNOWLEDGMENTS

We thank Amparo Ruiz-Prado for help with Arabidopsis propagation. This work was supported by Grants BB/H0024867/1, BB/I024496/1, BB/K015893/1, BB/L001276/1, and BB/M01133X/1 to M.R.B. from the Biotechnology and Biological Sciences Research Council, by a Ph.D. scholarship to B.Z. from the Chinese Scholarship Council, and by the Emmy Noether Fellowship of the Deutsche Forschungsgemeinschaft (Grant GR 4251/1-1 to C.G.).

AUTHOR CONTRIBUTIONS

R.K. designed the experimental strategies with M.R.B. R.K. and B.Z. carried out the SUS assays. C.G. and R.K. established the mOST4-anchored system for SEC11 interaction analysis in yeast. C.G. established the CytoSUS and Dex-inducible vectors. R.K. carried out the confocal studies and pull-downs with S.W. and immunoblot assays with C.A. B.Z., C.G., S.W., and R.K. designed constructs and vectors. R.K. and M.R.B. analyzed the data and wrote the article with support from C.G.

Received November 18, 2014; revised January 22, 2015; accepted February 15, 2015; published March 6, 2015.

REFERENCES

Aoyama, T., and Chua, N.H. (1997). A glucocorticoid-mediated transcriptional induction system in transgenic plants. Plant J. **11:** 605–612.

Archbold, J.K., Whitten, A.E., Hu, S.H., Collins, B.M., and Martin, J.L. (2014). SNARE-ing the structures of Sec1/Munc18 proteins. Curr. Opin. Struct. Biol. **29:** 44–51.

Assaad, F.F., Huet, Y., Mayer, U., and Jürgens, G. (2001). The cytokinesis gene KEULE encodes a Sec1 protein that binds the syntaxin KNOLLE. J. Cell Biol. **152:** 531–543.

Assaad, F.F., Qiu, J.L., Youngs, H., Ehrhardt, D., Zimmerli, L., Kalde, M., Wanner, G., Peck, S.C., Edwards, H., Ramonell, K., Somerville, C.R., and Thordal-Christensen, H. (2004). The PEN1 syntaxin defines a novel cellular compartment upon fungal attack and is required for the timely assembly of papillae. Mol. Biol. Cell **15:** 5118–5129.

Bassham, D.C., and Blatt, M.R. (2008). SNAREs: Cogs and coordinators in signaling and development. Plant Physiol. **147:** 1504–1515.

Besserer, A., Burnotte, E., Bienert, G.P., Chevalier, A.S., Errachid, A., Grefen, C., Blatt, M.R., and Chaumont, F. (2012). Selective regulation of maize plasma membrane aquaporin trafficking and activity by the SNARE SYP121. Plant Cell **24:** 3463–3481.

Blatt, M.R. (2000). Cellular signaling and volume control in stomatal movements in plants. Annu. Rev. Cell Dev. Biol. **16:** 221–241.

Blatt, M.R., and Grefen, C. (2014). Applications of fluorescent marker proteins in plant cell biology. In Arabidopsis Protocols, J.J. Sanchez-Serrano and J. Salinas, eds (New York: Humana Press), pp. 487–507.

Bock, J.B., Matern, H.T., Peden, A.A., and Scheller, R.H. (2001). A genomic perspective on membrane compartment organization. Nature **409:** 839–841.

Bracher, A., and Weissenhorn, W. (2002). Structural basis for the Golgi membrane recruitment of Sly1p by Sed5p. EMBO J. **21:** 6114–6124.

Burgoyne, R.D., and Morgan, A. (2007). Membrane trafficking: Three steps to fusion. Curr. Biol. **17:** R255–R258.

Campanoni, P., and Blatt, M.R. (2007). Membrane trafficking and polar growth in root hairs and pollen tubes. J. Exp. Bot. **58:** 65–74.

Christie, M.P., Whitten, A.E., King, G.J., Hu, S.-H., Jarrott, R.J., Chen, K.-E., Duff, A.P., Callow, P., Collins, B.M., James, D.E., and Martin, J.L. (2012). Low-resolution solution structures of Munc18:Syntaxin protein complexes indicate an open binding mode driven by the syntaxin N-peptide. Proc. Natl. Acad. Sci. USA **109:** 9816–9821.

Clough, S.J., and Bent, A.F. (1998). Floral dip: A simplified method for Agrobacterium-mediated transformation of *Arabidopsis thaliana*. Plant J. **16:** 735–743.

Demircioglu, F.E., Burkhardt, P., and Fasshauer, D. (2014). The SM protein Sly1 accelerates assembly of the ER-Golgi SNARE complex. Proc. Natl. Acad. Sci. USA **111:** 13828–13833.

Dulubova, I., Khvotchev, M., Liu, S., Huryeva, I., Südhof, T.C., and Rizo, J. (2007). Munc18-1 binds directly to the neuronal SNARE complex. Proc. Natl. Acad. Sci. USA **104:** 2697–2702.

Eisenach, C., Chen, Z.H., Grefen, C., and Blatt, M.R. (2012). The trafficking protein SYP121 of Arabidopsis connects programmed stomatal closure and K^+ channel activity with vegetative growth. Plant J. **69:** 241–251.

Enami, K., Ichikawa, M., Uemura, T., Kutsuna, N., Hasezawa, S., Nakagawa, T., Nakano, A., and Sato, M.H. (2009). Differential expression control and polarized distribution of plasma membrane-resident SYP1 SNAREs in *Arabidopsis thaliana*. Plant Cell Physiol. **50:** 280–289.

Fasshauer, D., Sutton, R.B., Brunger, A.T., and Jahn, R. (1998). Conserved structural features of the synaptic fusion complex: SNARE proteins reclassified as Q- and R-SNAREs. Proc. Natl. Acad. Sci. USA **95:** 15781–15786.

Furgason, M.L.M., MacDonald, C., Shanks, S.G., Ryder, S.P., Bryant, N.J., and Munson, M. (2009). The N-terminal peptide of the syntaxin Tlg2p modulates binding of its closed conformation to Vps45p. Proc. Natl. Acad. Sci. USA **106:** 14303–14308.

Geelen, D., Leyman, B., Batoko, H., Di Sansebastiano, G.P., Moore, I., and Blatt, M.R. (2002). The abscisic acid-related SNARE homolog NtSyr1 contributes to secretion and growth: Evidence from competition with its cytosolic domain. Plant Cell **14:** 387–406.

Grefen, C. (2014). The split-ubiquitin system for the analysis of three-component interactions. In Methods in Molecular Biology, J.J. Sanchez-Serrano and J. Salinas, eds (New York: Humana Press), pp. 659–673.

Grefen, C., and Blatt, M.R. (2008). SNAREs—Molecular governors in signalling and development. Curr. Opin. Plant Biol. **11:** 600–609.

Grefen, C., and Blatt, M.R. (2012a). A 2in1 cloning system enables ratiometric bimolecular fluorescence complementation (rBiFC). Biotechniques **53:** 311–314.

Grefen, C., and Blatt, M.R. (2012b). Do calcineurin B-like proteins interact independently of the serine threonine kinase CIPK23 with the K^+ channel AKT1? Lessons learned from a ménage à trois. Plant Physiol. **159:** 915–919.

Grefen, C., Chen, Z.H., Honsbein, A., Donald, N., Hills, A., and Blatt, M.R. (2010a). A novel motif essential for SNARE interaction with the K^+ channel KC1 and channel gating in *Arabidopsis*. Plant Cell **22:** 3076–3092.

Grefen, C., Donald, N., Hashimoto, K., Kudla, J., Schumacher, K., and Blatt, M.R. (2010b). A ubiquitin-10 promoter-based vector set for fluorescent protein tagging facilitates temporal stability and native protein distribution in transient and stable expression studies. Plant J. **64:** 355–365.

Grefen, C., Honsbein, A., and Blatt, M.R. (2011). Ion transport, membrane traffic and cellular volume control. Curr. Opin. Plant Biol. **14:** 332–339.

Grefen, C., Lalonde, S., and Obrdlik, P. (2007). Split-ubiquitin system for identifying protein-protein interactions in membrane and full-length proteins. Curr. Protoc. Neurosci. **Chapter 5:** 27.

Grefen, C., Obrdlik, P., and Harter, K. (2009). The determination of protein-protein interactions by the mating-based split-ubiquitin system (mbSUS). Methods Mol. Biol. **479:** 217–233.

Honsbein, A., Blatt, M.R., and Grefen, C. (2011). A molecular framework for coupling cellular volume and osmotic solute transport control. J. Exp. Bot. **62:** 2363–2370.

Honsbein, A., Sokolovski, S., Grefen, C., Campanoni, P., Pratelli, R., Paneque, M., Chen, Z.H., Johansson, I., and Blatt, M.R. (2009). A tripartite SNARE-K^+ channel complex mediates in channel-dependent K^+ nutrition in *Arabidopsis*. Plant Cell **21:** 2859–2877.

Hu, S.H., Christie, M.P., Saez, N.J., Latham, C.F., Jarrott, R., Lua, L.H.L., Collins, B.M., and Martin, J.L. (2011). Possible roles for Munc18-1 domain 3a and Syntaxin1 N-peptide and C-terminal anchor in SNARE complex formation. Proc. Natl. Acad. Sci. USA **108:** 1040–1045.

Hughson, F.M. (2013). Neuroscience. Chaperones that SNARE neurotransmitter release. Science **339:** 406–407.

Jahn, R., and Scheller, R.H. (2006). SNAREs—Engines for membrane fusion. Nat. Rev. Mol. Cell Biol. **7:** 631–643.

Kalde, M., Nühse, T.S., Findlay, K., and Peck, S.C. (2007). The syntaxin SYP132 contributes to plant resistance against bacteria and secretion of pathogenesis-related protein 1. Proc. Natl. Acad. Sci. USA **104:** 11850–11855.

Karnik, A., Karnik, R., and Grefen, C. (2013a). SDM-Assist software to design site-directed mutagenesis primers introducing "silent" restriction sites. BMC Bioinformatics **14:** 105.

Karnik, R., Grefen, C., Bayne, R., Honsbein, A., Köhler, T., Kioumourtzoglou, D., Williams, M., Bryant, N.J., and Blatt, M.R.

(2013b). *Arabidopsis* Sec1/Munc18 protein SEC11 is a competitive and dynamic modulator of SNARE binding and SYP121-dependent vesicle traffic. Plant Cell **25:** 1368–1382.

Khvotchev, M., Dulubova, I., Sun, J., Dai, H., Rizo, J., and Südhof, T.C. (2007). Dual modes of Munc18-1/SNARE interactions are coupled by functionally critical binding to syntaxin-1 N terminus. J. Neurosci. **27:** 12147–12155.

Kwon, C., et al. (2008). Co-option of a default secretory pathway for plant immune responses. Nature **451:** 835–840.

Lauber, M.H., Waizenegger, I., Steinmann, T., Schwarz, H., Mayer, U., Hwang, I., Lukowitz, W., and Jürgens, G. (1997). The Arabidopsis KNOLLE protein is a cytokinesis-specific syntaxin. J. Cell Biol. **139:** 1485–1493.

Leyman, B., Geelen, D., Quintero, F.J., and Blatt, M.R. (1999). A tobacco syntaxin with a role in hormonal control of guard cell ion channels. Science **283:** 537–540.

Lipka, E., Gadeyne, A., Stöckle, D., Zimmermann, S., De Jaeger, G., Ehrhardt, D.W., Kirik, V., Van Damme, D., and Müller, S. (2014). The Phragmoplast-Orienting Kinesin-12 class proteins translate the positional information of the preprophase band to establish the cortical division zone in *Arabidopsis thaliana*. Plant Cell **26:** 2617–2632.

Lipka, V., Kwon, C., and Panstruga, R. (2007). SNARE-ware: The role of SNARE-domain proteins in plant biology. Annu. Rev. Cell Dev. Biol. **23:** 147–174.

Misura, K.M.S., Scheller, R.H., and Weis, W.I. (2000). Three-dimensional structure of the neuronal-Sec1-syntaxin 1a complex. Nature **404:** 355–362.

Misura, K.M.S., Scheller, R.H., and Weis, W.I. (2001). Self-association of the H3 region of syntaxin 1A. Implications for intermediates in SNARE complex assembly. J. Biol. Chem. **276:** 13273–13282.

Möckli, N., Deplazes, A., Hassa, P.O., Zhang, Z., Peter, M., Hottiger, M.O., Stagljar, I., and Auerbach, D. (2007). Yeast split-ubiquitin-based cytosolic screening system to detect interactions between transcriptionally active proteins. Biotechniques **42:** 725–730.

Muller, I., Wagner, W., Volker, A., Schellmann, S., Nacry, P., Kuttner, F., Schwarz-Sommer, Z., Mayer, U., and Jurgens, G. (2003). Syntaxin specificity of cytokinesis in Arabidopsis. Nat. Cell Biol. **5:** 531–534.

Obrdlik, P., et al. (2004). K^+ channel interactions detected by a genetic system optimized for systematic studies of membrane protein interactions. Proc. Natl. Acad. Sci. USA **101:** 12242–12247.

Pajonk, S., Kwon, C., Clemens, N., Panstruga, R., and Schulze-Lefert, P. (2008). Activity determinants and functional specialization of Arabidopsis PEN1 syntaxin in innate immunity. J. Biol. Chem. **283:** 26974–26984.

Park, M., Touihri, S., Müller, I., Mayer, U., and Jürgens, G. (2012). Sec1/Munc18 protein stabilizes fusion-competent syntaxin for membrane fusion in Arabidopsis cytokinesis. Dev. Cell **22:** 989–1000.

Pratelli, R., Sutter, J.U., and Blatt, M.R. (2004). A new catch in the SNARE. Trends Plant Sci. **9:** 187–195.

Rathore, S.S., Bend, E.G., Yu, H., Hammarlund, M., Jorgensen, E.M., and Shen, J. (2010). Syntaxin N-terminal peptide motif is an initiation factor for the assembly of the SNARE-Sec1/Munc18 membrane fusion complex. Proc. Natl. Acad. Sci. USA **107:** 22399–22406.

Rehman, R.U., Stigliano, E., Lycett, G.W., Sticher, L., Sbano, F., Faraco, M., Dalessandro, G., and Di Sansebastiano, G.P. (2008). Tomato Rab11a characterization evidenced a difference between SYP121-dependent and SYP122-dependent exocytosis. Plant Cell Physiol. **49:** 751–766.

Reichardt, I., Slane, D., El Kasmi, F., Knöll, C., Fuchs, R., Mayer, U., Lipka, V., and Jürgens, G. (2011). Mechanisms of functional specificity among plasma-membrane syntaxins in Arabidopsis. Traffic **12:** 1269–1280.

Rizo, J., and Südhof, T.C. (2012). The membrane fusion enigma: SNAREs, Sec1/Munc18 proteins, and their accomplices—Guilty as charged? Annu. Rev. Cell Dev. Biol. **28:** 279–308.

Sanderfoot, A.A., Assaad, F.F., and Raikhel, N.V. (2000). The Arabidopsis genome. An abundance of soluble N-ethylmaleimide-sensitive factor adaptor protein receptors. Plant Physiol. **124:** 1558–1569.

Shope, J.C., DeWald, D.B., and Mott, K.A. (2003). Changes in surface area of intact guard cells are correlated with membrane internalization. Plant Physiol. **133:** 1314–1321.

Sieber, J.J., Willig, K.I., Kutzner, C., Gerding-Reimers, C., Harke, B., Donnert, G., Rammner, B., Eggeling, C., Hell, S.W., Grubmüller, H., and Lang, T. (2007). Anatomy and dynamics of a supramolecular membrane protein cluster. Science **317:** 1072–1076.

Sollner, R., Glasser, G., Wanner, G., Somerville, C.R., Jurgens, G., and Assaad, F.F. (2002). Cytokinesis-defective mutants of Arabidopsis. Plant Physiol. **129:** 678–690.

Südhof, T.C., and Rothman, J.E. (2009). Membrane fusion: Grappling with SNARE and SM proteins. Science **323:** 474–477.

Sutter, J.U., Campanoni, P., Tyrrell, M., and Blatt, M.R. (2006). Selective mobility and sensitivity to SNAREs is exhibited by the *Arabidopsis* KAT1 K^+ channel at the plasma membrane. Plant Cell **18:** 935–954.

Sutter, J.U., Sieben, C., Hartel, A., Eisenach, C., Thiel, G., and Blatt, M.R. (2007). Abscisic acid triggers the endocytosis of the Arabidopsis KAT1 K^+ channel and its recycling to the plasma membrane. Curr. Biol. **17:** 1396–1402.

Tyrrell, M., Campanoni, P., Sutter, J.U., Pratelli, R., Paneque, M., Sokolovski, S., and Blatt, M.R. (2007). Selective targeting of plasma membrane and tonoplast traffic by inhibitory (dominant-negative) SNARE fragments. Plant J. **51:** 1099–1115.

Uemura, T., Ueda, T., Ohniwa, R.L., Nakano, A., Takeyasu, K., and Sato, M.H. (2004). Systematic analysis of SNARE molecules in Arabidopsis: Dissection of the post-Golgi network in plant cells. Cell Struct. Funct. **29:** 49–65.

Waizenegger, I., Lukowitz, W., Assaad, F., Schwarz, H., Jürgens, G., and Mayer, U. (2000). The Arabidopsis KNOLLE and KEULE genes interact to promote vesicle fusion during cytokinesis. Curr. Biol. **10:** 1371–1374.

Walter, A., Silk, W.K., and Schurr, U. (2009). Environmental effects on spatial and temporal patterns of leaf and root growth. Annu. Rev. Plant Biol. **60:** 279–304.

Yun, H.S., Kwaaitaal, M., Kato, N., Yi, C., Park, S., Sato, M.H., Schulze-Lefert, P., and Kwon, C. (2013). Requirement of vesicle-associated membrane protein 721 and 722 for sustained growth during immune responses in Arabidopsis. Mol. Cells **35:** 481–488.

Zhang, Z., Feechan, A., Pedersen, C., Newman, M.A., Qiu, J.L., Olesen, K.L., and Thordal-Christensen, H. (2007). A SNARE-protein has opposing functions in penetration resistance and defence signalling pathways. Plant J. **49:** 302–312.